Georgia State University
ScholarWorks @ Georgia State University

Computer Science Theses | Department of Computer Science

8-8-2023

Geant4 Simulation for Radon Propagation in Soil

Mayur P. Aitavadekar
Georgia State University

Follow this and additional works at: https://scholarworks.gsu.edu/cs_theses

Recommended Citation

Aitavadekar, Mayur P., "Geant4 Simulation for Radon Propagation in Soil." Thesis, Georgia State University, 2023.
https://scholarworks.gsu.edu/cs_theses/109

This Thesis is brought to you for free and open access by the Department of Computer Science at ScholarWorks @ Georgia State University. It has been accepted for inclusion in Computer Science Theses by an authorized administrator of ScholarWorks @ Georgia State University. For more information, please contact scholarworks@gsu.edu.

Geant4 Simulation for Radon Propagation in Soil

by

Mayur Aitavadekar

Under the Direction of Ashwin Ashok, Ph.D. and Xiaochun He. Ph.D.

A Thesis Submitted in Partial Fulfillment of the Requirements for the Degree of

Master of Science

in the College of Arts and Sciences

Georgia State University

2023

ABSTRACT

Radon is a radioactive element in the periodic table that is generated from the decay of radium below the earth's surface. After a generation, it travels through the soil and reaches the earth's surface. Radon poses a radiological health risk. Therefore, the research community pays close attention to radon.

This thesis reviews the complete process of radon propagation from soil to air and studies the effects of different environmental and geological parameters which influence radon flux. A Geant4 simulation program based on C++ has been developed to study radon propagation in soil. The process of simulation setup and the results of this simulation study will provide detailed knowledge of the effect of moisture content and grain size on the radon emanation coefficient. Apart from the simulation, the analysis of data gathered by the experimental setup of Geiger counters deployed at Stone Mountain is provided.

INDEX WORDS: Radon, Geant4, C++, OpenRadon Lab, Geiger Counters, ROOT.

Copyright by
Mayur Aitavadekar
2023

Geant4 Simulation for Radon Propagation in Soil

by

Mayur Aitavadekar

Committee Chairs: Ashwin Ashok

Xiaochun He

Committee: Nadine Kabengi

Anu Bourgeois

Electronic Version Approved:

Office of Graduate Studies

College of Arts and Sciences

Georgia State University

August 2023

ACKNOWLEDGEMENTS

When I entered the M.S. in Computer Science program at Georgia State University (GSU), I could not have imagined that I would study Geology and Physics as well. At first, I thought that I would learn computer science as I had planned. Life has been a bit more hectic than that. But it has been fun.

My four semesters at GSU have been delightful because of the people I have come to know. Throughout this period, Dr. Xiachun He has meant many things to me. Dr. Xiachun has spent patient hours with me in Lab 256 at Natural Science Center, unraveling our research direction and simplifying my disoriented thoughts. He truly taught me how to be creative and do research. I am deeply indebted to him.

Dr. Ashwin gave me a unique opportunity to work on an interdisciplinary topic. As an academic advisor, Dr. Ashwin constantly motivated me to move forward in our research endeavors. Since the beginning, He knew that we are solving a tough problem. Therefore, he has been patient throughout the period. I cannot thank him enough for awarding me a graduate research assistantship for my master's degree which was completely funded by a USDA grant 2021-67019-34337.

Dr. Nadine's enthusiasm has made much of this work enjoyable. Geology was never my forte and therefore it was very hard for me to tackle Dr. Nadine's questions. In discussions, she throws very important questions which can shape your research. I regret I could not work more in person with Dr. Nadine.

I genuinely want to thank Dr. Anu for being a member of my committee. She was kind enough to accept my request.

My mother and father are an inspiration for this thesis. Their hard work always motivated me. My sister always affectionately asked me about my research. My family's patience and support have been immense. Everything I am, I owe to them and I dedicate this work to them.

TABLE OF CONTENTS

LIST OF TABLES

LIST OF FIGURES

1 INTRODUCTION

Radon(^{222}Rn) is the heaviest noble element in the periodic table and it is radioactive, inert, colorless, and odorless. In the uranium(^{238}U) decay chain, the radioactive decay of radium(^{226}Ra) produces radon. Uranium is the primary source of radon since the entire decay chain starts from uranium. During radioactive decay, physical reactions involving subatomic particles at the atomic or nuclear level always result in ionizing radiation [6] that is harmful to human health. Radon is the predominant cause of the public's exposure to natural ionizing radiation [9]. Due to this health hazard, a lot of attention is given to radon as a health hazard. The scientific studies by the World Health Organization imply that there is a relation between indoor radon exposure and lung cancer [10]. Hence, in recent years, many studies have been conducted on radon.

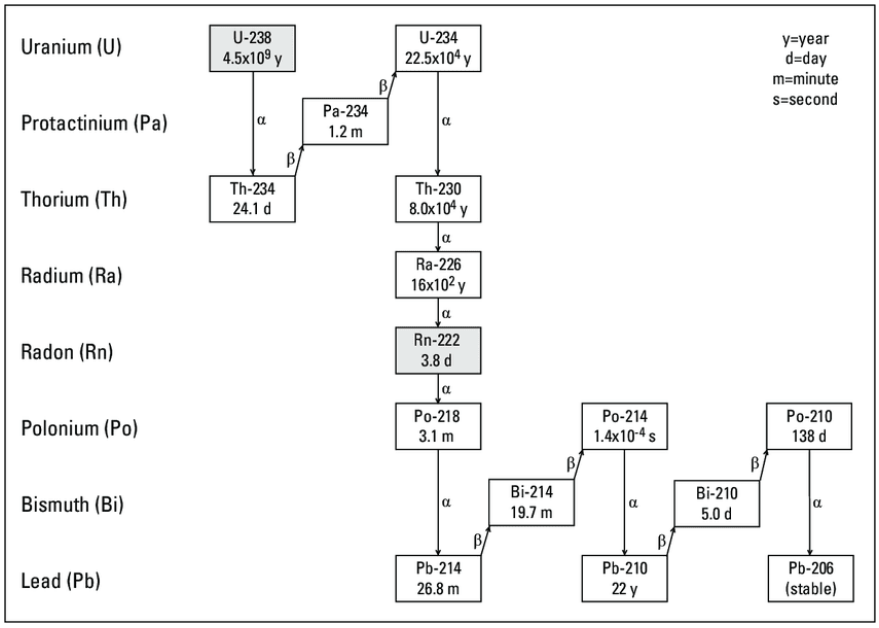

Figure 1.1: Uranium−238 Decay Chain

As shown in Fig. 1.1, radium is the direct source of radon generation because radium undergoes alpha decay to form radon. During alpha decay, an unstable nucleus is converted into another element by kicking out a particle composed of two protons and two neutrons from itself. As shown below radium undergoes alpha decay to form radon [11].

$$^{226}_{88}\mathrm{Ra} \longrightarrow {}^{222}_{86}\mathrm{Rn} + {}^{4}_{2}\mathrm{He} + \text{energy}$$

Radon itself is not harmful to humans directly. But, during its radioactivity, it undergoes alpha decay as shown below:

$$^{222}_{86}\mathrm{Rn} \longrightarrow {}^{218}_{84}\mathrm{Po} + {}^{4}_{2}\mathrm{He} + \text{energy}$$

^{218}Po and alpha particles are short-lived decay products. These constitute primary health concerns. ^{218}Po is very reactive and has a life of 3.04 minutes. Alpha particles carry large mass, hence they do not travel long distances in the air or go deep into solids. Yet, they can damage internal tissues when they enter the body. There are three isotopes of Radon- ^{222}Rn (shown in Fig. 1.1), ^{220}Rn, and ^{219}Rn. ^{220}Rn is generated in ^{232}Th decay chain and ^{29}Rn is generated in ^{236}U decay chain. But out of these three isotopes, the research community focuses more on ^{222}Rn because it is responsible for the largest radiation dose.

With this thesis, we aim to study ^{222}Rn propagation through the soil by developing a realistic simulation. Hence, to achieve our goal, this thesis is organized as follows:

1. We want to understand Radon flux on the surface of the earth under various geological parameters, and environmental factors. Hence, to study Radon propagation through the soil, we need to properly understand the various properties of Radon in soil, how radon particles reach the surface of the earth, and the various stages of radon propagation. Chapter 2 provides a literature review related to these topics. It further explains the effects of various soil characteristics on Radon propagation. Chapter 2 contains qualitative and quantitative information that will be useful for us in developing a simulation study.

2. To understand actual radon flux coming at the surface, a Radon testbed has been developed by the GSU OpenRadon Lab. We have deployed Radon measurement devices that continuously take measurements of Radon flux at different depths. We have also deployed Geiger counters that measure background radiation data. Chapter 3 provides brief information about the radon testbed.

3. The core contribution of this thesis is the simulation for Radon propagation. After understanding Radon transport through the soil in Chapter 2 and having a general understanding of the Radon testbed that provides Radon and background radiation measurements, a Geant4-based simulation has been developed to study radon propagation at the microscopic level. Chapter 4 details the research progress; it includes an introduction to Geant4, the simulation setup, the use of a literature review, data analyses, and an overview of the challenges encountered in the simulation development.

4. Chapter 5 summarizes the work completed and offers a future outlook for this research.

2 RADON PROPAGATION THROUGH SOIL

2.1 Process of Radon Propagation

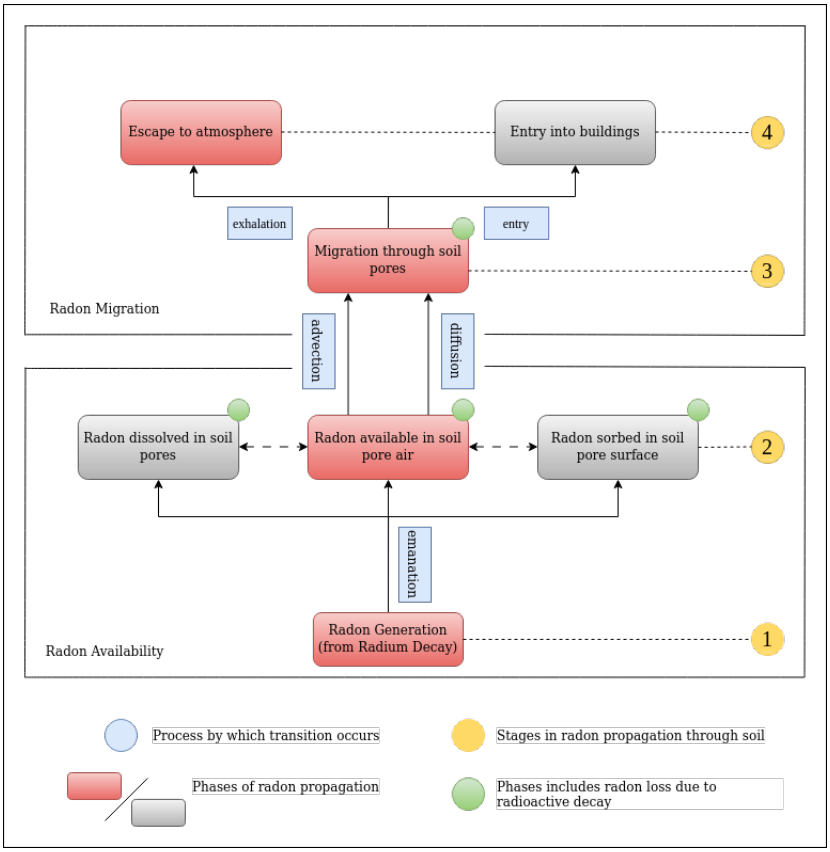

Figure 2.1: Schematic representation of radon propagation from soil to the atmosphere as explained in *W. W. Nazaroff et al., Radon transport from soil to air* paper [1]. The phases in red color are considered important during the development of the simulation. The horizontal dashed arrows in Stage 2 indicate that transitions between the three phases may occur due to environmental parameters such as moisture and temperature.

As shown in Fig. 2.1, the entire process of radon propagation is divided into two main clusters: 1) Radon availability, and 2) Radon migration. The process of radon propagation is divided into four stages; each stage has phase(s) shown in red or gray boxes. Since the goal of the thesis is to understand radon propagation, phase(s) in a red-colored box are considered significant during the development of the simulation.

Table 2.1 shows processes and parameters associated with each process by which transition occurs from one phase into another.

Table 2.1: Process by which transition occurs from one stage to the other and corresponding parameters associated with each process.

Process	**Parameters**
emanation	moisture, temperature, grain size, location of radon atoms
advection	intrinsic soil permeability, moisture, pressure gradient
diffusion	moisture, porosity, tortuosity
exhalation	diffusive transport, wind, barometric pressure changes
entry	temperature differences, wind, barometric pressure changes, substructure type, quality of construction, fan operation

Stage ① includes the phenomenon of radon generation due to Radioactive decay and its availability in earth's crust. Stage ② explains the existence of radon in different mediums such as dissolved in water, available in air, and/or sorbed on soil pore surface (from left to right). Stage ③ explains the migration of radon through soil pores due to various geological parameters that significantly contribute to radon propagation. Stage ④ is final

stage where after migration through stage ③ radon finally enters either in atmosphere(above earth surface) or in buildings.

2.1.1 Stage 1 - Radon generation

We have already seen that radon is generated by the alpha decay of radium. Radium is found in soil and rock. This radium content is expressed in terms of activity concentration per unit mass. Since radon is produced from radium, this radium activity concentration is equivalent to a production rate of radon in the soil [1]. Activity concentrations are typically measured in Ci(Curie) and/or Bq(Becquerel). 1 Ci is equivalent to 3.7×10^{10} Bq.

Although radon is directly generated from radium Decay, uranium is considered the ultimate source of radon since it is observed in the Decay chain of uranium. Therefore, to understand the availability of radon in the soil we must understand the availability of Uranium. The general unit for measurement of uranium in Rocks and/or soil is ppm (parts per million). All rocks contain uranium but most of them contain very small amounts like 1-3 ppm which is a very small amount. Eventually, the rocks are converted into the soil by geochemical processes. Hence, we can say that typical soil has 1-3 ppm of Uranium. Some rocks that exist in the earth's crust have almost 100 ppm of uranium. This is comparatively high compared to the typical concentration of uranium. It is obvious that the higher the uranium level in the soil below the earth's surface in a particular area, Greater will be the chances to find radon above that earth's surface's air [12].

Figure 2.2: Sample of uranium ore (Source: Google Images)

As stated in Chapter 1, radium alpha decay plays a vital role in radon generation and its availability in soil. When radium is converted into radon, an alpha particle is created and this alpha particle carries some energy which we call alpha recoil. Because of this recoil, radon particle moves in the opposite direction of recoil [13]. Because of this, there are few number of possible locations where radon particles might move. We explain radon particle movement due to alpha recoil in the following Stage ②.

2.1.2 Stage 2 - Radon emanation and availability in various mediums

After the alpha decay of radium, only a fraction of radon generated in the soil grain leaves the soil grain and enters the pore volume of the soil. This fraction of radon that escapes the soil grain is called “emanation coefficient”, ”emanating fraction” or ”emanating power” [1].

Alpha decay of radium follows the conservation of momentum and energy. The kinetic energy of a radon particle just after its generation is 86 keV. We used this while during the

implementation of the simulation. In Chapter 4, we will verify this energy value in more detail through theoretical calculations.

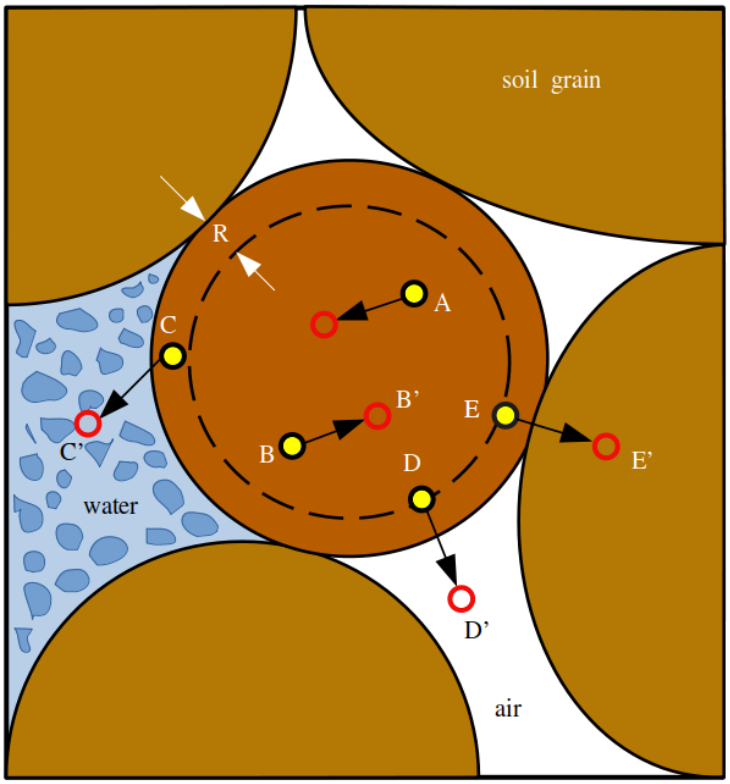

Figure 2.3: Schematic representation of radon emanation. The yellow circle denotes the location of the radium atom which decays into an alpha particle and produces a radon atom that travels a certain distance due to recoil and stops at a point denoted by a red circle. The dashed circular line represents recoil range R.

The important question is - after the decay of radium, followed by the generation of radon how far will radon particle travel, and where will it finally stop after traveling? To answer this question, we will take reference of Fig. 2.3 to understand the following cases:

1. When the radium atom is inside recoil range R, we can say that it is deeply embedded inside soil grain as shown Fig. 2.3 at points A and B. In this case, a radon atom will travel a very short distance such as points A′ and B′. It will remain inside the soil grain.

2. When the radium atom is on/outside the recoil range R (dashed line shown in Fig. 2.3), there is a high possibility that it will travel outside the soil grain. Hence, the following possibilities for travel arise:

   (a) Consider point C where a radon atom has entered in pore space filled with water at a point C′. It is dissolved in water.

   (b) Consider point D where radon atom has entered in pore space with air at point D′. Only in this case radon migration can occur.

   (c) Consider point E where radon atom has entered in neighboring soil grain at point E′. It gets embedded in neighboring soil grain.

The destination location of the radon atom depends upon the direction of the recoil, the moisture level of soil grains, the average dimension of soil pore, and the size of soil grains. It is important to know that what are the values of the recoil range R. These values can be very much important while developing the simulation study. Based on [14], the following are the values of recoil range R in different mediums in soil: (1) 63 um in air, (2) 0.1 um in water, and (3) 0.02-0.07 um in common minerals.

Except for case 2(b), in all other cases, the radon atom will not be moved. This is because we mainly consider the movement of radon to be a gaseous phase. Gases can move much better in a gaseous medium(like air) than in liquid(water) or solid(mineral grains). The air provides much less resistance to the movement of radon. Therefore, only when a radon atom enters an air medium, radon migration will occur.

As shown in Fig. 2.1, the solid dashed line indicates that a transition between the three phases might occur due to geological parameters like moisture, temperature, etc. In Section 2.2, we will see in detail what are the different parameters which affect radon emanation in soil grain and the scientific reasoning behind it. For now, we only understand that this transition can occur. Following are some important points we need to keep in mind:

1. When radon is embedded in soil grain or dissolved in water, diffusion from these phases to the gas phase (although very negligible) can happen. But this transition is very slow.

2. Similarly, when radon is free in the air, during migration it can get sorbed on other surfaces of other soil grains, or if after traveling some distance the water is present in soil pores, it may get dissolved in that water.

Next, stage ③ explains radon migration. To explain radon migration, we will study the theory of radon migration as well as mathematical models developed by the research community over the years. We will go through these concepts in detail in stage ③.

2.1.3 Stage 3 - Radon migration through soil pores

The primary aim of the thesis is to understand radon propagation through the soil. Hence, understanding of stage ③ is very important for us. Although we will discuss core concepts about transport mechanisms for radon migration, in Chapter 4, we will discuss challenges in applying these transport mechanisms in our simulation.

Radon migration through soil pores can happen because of two types of transport mechanisms: 1) diffusive transport, and 2) advective transport. Let's discuss both of the transport mechanisms in detail.

Diffusive transport: The molecular motion from the region of high concentration to the region of low concentration is known as 'diffusion'. Since radon in the migration stage occurs in a gaseous state, it follows a diffusion mechanism for propagation through the soil pores. Radon transport in soil occurs mainly due to diffusion [15]. The flux density of radon is nothing but the number of radon atoms passing through per unit area. The flux density due to diffusion is mathematically described by Fick's law which is written as:

$$J^d = -D_0 \cdot \nabla \cdot I_a \tag{2.1}$$

where J^d is radon flux density(Bq m^{-2} s^{-2}) in a region due to diffusion. D_0 is diffussion coefficient(m^2 s^{-1}). I_a is an activity concentration of radon present in the soil(Bqm^3). ∇ is gradient operator(m^{-1}). Although Fick's law applies to the diffusive transport of radon,

we must understand that there is no fixed standard way to write Fick's law for diffusion in porous media. Differences in various works can arise when concentrations or fluxes are written in terms of total volume or area instead of air-filled soil pore area or volume.

The value of the diffusion coefficient is used in various mathematical equations related to radon transport. It can be very useful for us in the future to make important calculations.

Table 2.2: Diffusion coefficient values for radon in the soil as mentioned in paper [1].

Soil description	D_0	**Important remarks**
Uranium tailings	range of $(5.4 - 7.1)$ x 10^{-6}	moisture content=0.7-1.5%
Silty sandy clay	2.7 x 10^{-6}	moisture content=1.5%
	2.5 x 10^{-7}	moisture content=10.5%
	6.0 x 10^{-8}	moisture content=17.3%
Compacted silty sands	3.0 ± 1.3 x 10^{-6}	porosity=0.29-0.41
Compacted clay sands	3.2 ± 1.5 x 10^{-6}	porosity=0.32-0.39
Compacted inorganic clays	2.5 ± 1.0 x 10^{-6}	porosity=0.32-0.43

The effective diffusion coefficient of radon in the soil of low moisture content is 3 x 10^{-6} m^{-2} s^{-2}. This is a factor of 4 smaller than the diffusion coefficient value in air [1]. In saturated soil where water content is more in soil, the radon diffusion coefficient is 2 x 10^{-10} m^{-2} s^{-2}. This is a very low value. We can say that water blocks the radon diffusion in soil pores. But if you think deeply, this is not always true since radon can be dissolved in water and travel very slowly through it over time. But for practical purposes, we can assume that

more water content blocks radon diffusion in soil pores. The next transport mechanism for radon propagation is advective transport.

Advective transport: Advection is the transport of matter by the motion of the fluid. While matter moves with the fluid, its properties remain unchanged. Fluid may be any material that contains thermal energy such as water or air [16].

Advective transport is mathematically described by Dick's law which is written as follows:

$$V_D = -(k/\mu) \cdot \nabla P \tag{2.2}$$

Where V_D is the superficial velocity vector of fluid. It is the volumetric flow per unit total cross-sectional area. k is the intrinsic permeability of the soil. μ dynamic viscosity of fluid. ∇P is gradient of dynamic pressure(total pressure minus hydrostatic component) [1].

It is important to note that if we want to use an advective transport mechanism in our simulation, we need to keep in mind some important points explained in paper [1] as follows:

1. Pore size developed in the simulation must be large as compared relative mean free path of moving radon particles as well as fluid(in our case air).

2. For our simulation setup, we have an air medium in the soil pore area. So given superficial air velocity through the soil, the radon activity per unit of pore air area due to advective air flow is expressed as follows:

$$J^d = \frac{I_a \cdot V_D}{\varepsilon_a} \tag{2.3}$$

3. If we combine Eq. 2.2 with the continuity equation and equation of state, we can get governing equation for dynamic pressure in the soil. We can solve this governing equation for our geometry in simulation with appropriate boundary conditions on dynamic pressure to determine advective velocity in the soil.

We have discussed two transport mechanisms that govern radon propagation in soil pores. In Chapter 4, we will discuss how knowledge of these transport mechanisms is useful for the development of simulation, what are the different challenges in applying these concepts in the simulation, and what assumptions we are making in applying these concepts.

2.1.4 Stage 4 - Radon entry in atmosphere

We have discussed three stages of the radon propagation model as shown in Fig. 2.1. From its generation, it travels through soil layers and finally reaches above the earth's surface i.e. atmosphere. This is the final stage in our radon propagation model. There are two phases in this stage - 1) Escape to a free atmosphere, and 2) Entry into buildings.

Both of these phases have a vast scope of scientific literature review. When we study radon entry into the building, we need to understand mathematical representations of how radon is related to building materials, concepts of ventilation and how it affects the radon flow, heating and air-conditioning systems, and concepts of substructure, etc. All of these topics are beyond the scope of the thesis. Therefore, we will not go into the details of these phases since our thesis does focus on what happens when radon escapes to the atmosphere or how it enters into buildings.

Now that we have understood the entire radon propagation model, in Section 2.2, we will study how surface radon flux varies with various environmental and geological parameters. These are nothing but studies of the correlation between radon and particular parameter. The information in Section 2.2 is taken from various scientific papers in the radon research community.

2.2 Factors affecting Radon Propagation

This section briefly explains the correlation between radon and different environmental parameters. We also explain the logical reasoning behind the correlations wherever necessary.

2.2.1 Effect of moisture content on radon emanation

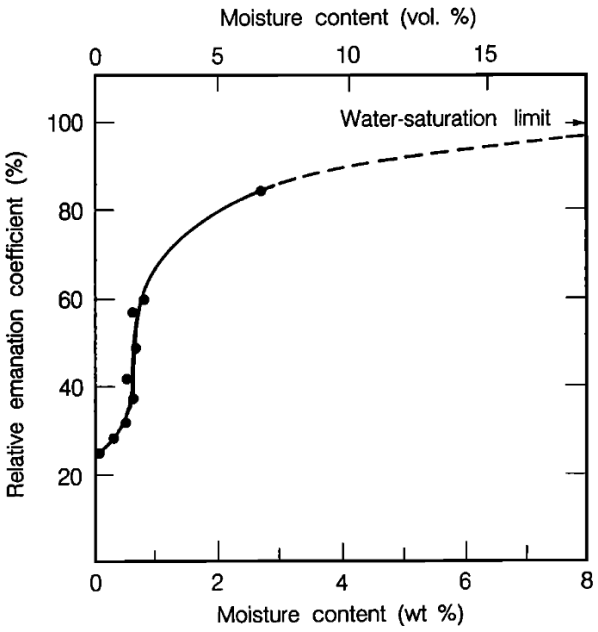

Figure 2.4: Effect of moisture content on relative radon emanation coefficient for a sample of uranium mill tailings (taken from [4]).

The moisture content has a very good correlation with the radon emanation coefficient. As the moisture content in the soil increases, the radon emanation coefficient increases. Studies show that radon emanation is much higher if the source material is moist or wet rather than dry. This is simply because the recoil range of radon is greater in water than in minerals. Radon emanation from soil grain is significantly impacted by the amount of water content in the soil.

2.2.2 Effect of the chemical composition of soil on radon emanation

The paper [6] shows a correlation between different chemical elements in soil and radon at $p\text{-}value < 0.05$. The presence of chemical elements Fe, Al, Mn, Si, and Ra in the soil increases the radon emanation coefficient. Experimental results show that the correlation coefficient between Mn content and emanation coefficient is approximately 0.4. The further

correlation coefficient between Fe content and radon emanation coefficient is approximately 0.8. Hence radon emanation coefficient is proportional to the Fe content in the soil.

Fe-oxyhydroxide and Mn-oxyhydroxide have a great ability to absorb radium [5]. Hence if they are present in soil grain they can adsorb Radium and therefore radium atoms can be distributed over the surface of the grain. So if the radium is distributed on the surface already radon produced after alpha decay will directly be present in the soil pore area. This phenomenon increases radon emanation.

2.2.3 Effect of pH of the soil on radon emanation

As per experimental results, radon emanation is well correlated with the pH (4-8) of the soil with a correlation coefficient of approximately 0.6 [6]. The reason for this good correlation is the same as mentioned in section 2.2.2. Between pH values 4-8, the Fe/Mn oxides or oxyhydroxides have a higher capacity for the adsorption of radium.

2.2.4 Effect of moisture content on radon diffusion

Radon diffusion is significantly impacted by the water content in the soil. We have already discussed the reasons for this effect. Moisture content is inversely correlated with radon diffusion. As moisture content increases, radon diffusion decreases. The radon propagation is very high in the air as compared to water. So water acts as a blocking medium for radon propagation through soil pores. Because of more moisture content, the gap size between soil grains is decreased since water holds the soil grains tightly together. Hence it blocks radon diffusion.

2.2.5 Effect of temperature change on radon diffusion

The temperature of the soil is well correlated with radon diffusion. For example, radon diffusion at 100 °C is 7 times higher than radon diffusion at 25 °C which is room temperature. Due to an increase in temperature, the pressure gradient is created in the soil pores which results in advective gas flow [6].

The theory of advective transport mechanism is applicable in this case which is discussed in section 2.1.3. From Eq. (2.2) we can say that:

$$V_D \propto \nabla P \ , \tag{2.4}$$

where V_D is the velocity vector of fluid in soil pores which can be air or water. ∇P is pressure gradient. As the pressure gradient increases due to an increase in temperature, From Eq.(2.4), we can say that the velocity of the fluid in soil pores will increase. Due to this advective flow, from Eq.(2.3) we can say that:

$$J_d \propto V_D \ , \tag{2.5}$$

where J_d is radon flux through the unit area due to the velocity vector of fluid V_D. From Eq.(2.4) and Eq.(2.5), we can conclude that:

$$J_d \propto \nabla P \tag{2.6}$$

Hence radon flux is proportional to the pressure gradient formed in soil pores due to an increase in temperature. Therefore, the greater the temperature more will be pressure gradient which ultimately increases radon diffusion.

3 RADON TEST BED

3.1 OpenRadon Lab

OpenRadon Lab [9] is a comprehensive test bed developed at Georgia State University to study radon data. OpenRadon Lab uses the following approach to study the properties of radon:

1. Review the theoretical properties of soil and study physical, chemical, and geological parameters using samples collected at the site of the radon test bed.
2. Develop a realistic simulation of Radon propagation through soil layers
3. Measure the actual data at the site of the radon test bed and perform data-driven empirical modeling.

3.2 OpenRadon Lab Deployment

For the simulation study of radon propagation, we have made two deployments- 1) Sensor nest grid, and 2) Geiger-Muller Counter. Let's understand what are these deployments and what is their usage.

3.2.1 Sensor nest grid

Sensor Nest is one of the most important components of OpenRadon Lab. Sensor Nest is a well-tested and waterproof box that contains a commercial air-quality sensor. This sensor measures air-diffused radon, carbon dioxide, pressure, temperature, volatile organic compounds, and relative humidity [9].

Figure 3.1: Radon testbed at Stone Mountain, GA, USA.

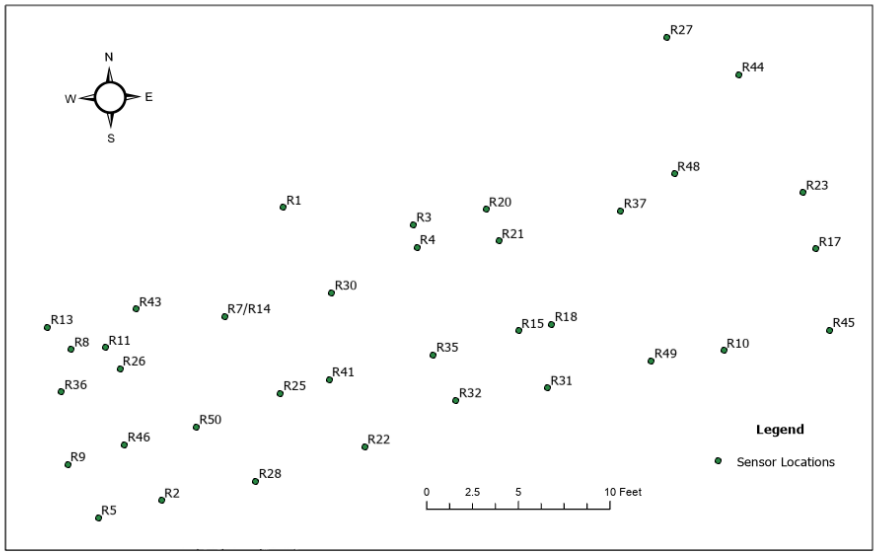

Figure 3.2: Schematic representation of sensor grid at Stone Mountain, GA, USA. (Credits: Soumya Tasmin, MS Candidate, Department of Geosciences, Georgia State University, Atlanta, GA 30324.)

We have deployed 40 Sensor Nodes at Stone Mountain Park in Dekalb County of Georgia. Fig. 3.2 schematic representation of sensor nest node grid deployed at Stone Mountain Park in Dekalb County of Georgia. Most of the nodes(blue-colored) are deployed at a depth of 5 ft. below the ground. Sensor node *R29* and *R19* are deployed at 3 ft. below the ground. Sensor node *R16* and *R39* are deployed at 6 in. below the ground.

We need to understand the radon flux variation at different depths as well. Therefore we have placed a few sensor nodes at different depths. The aim is to understand spatiotemporal variation in radon flux so all of the remaining nodes are placed at equal depth.

Sensor nest grid provides time series data of radon flux along with other parameters such as temperature, pressure, humidity, etc. The values of these parameters are very important while developing a simulation study.

3.2.2 Development of geiger counter setup

(A) (B) (C)

Figure 3.3: (A) Geiger counter with white Geiger-Muller tube on top of it. (B) IoT setup for Geiger counts measurement

Geiger-Muller counter or simply the Geiger counter is sensitive to background radiation. More specifically, these are electronic instruments that are used for detecting and measuring ionizing radiations. A few examples of ionizing radiation are- radiation due to Alpha particles, radiation due to Beta particles, radiation due to Gamma rays, etc. In the research community, Geiger counters are known as the world's best-known radiation detection instruments.

Fig. 3.3 shows our setup for the Geiger counter. In Fig. 3.3(A), we have a Geiger counter with a Geiger-Muller tube on top of it. This tube captures ionizing radiation when a particle travels through it. The following are the primary reasons for Geiger counter deployment at Stone Mountain Park:

1. Geiger counter is sensitive to background radiation which includes gamma and beta particles from the nearby environments (soil, brick, and concrete, mainly) and radiation from cosmic ray showers.

2. Radon is generated from radioactive decay from the same source of radiation in soil, brick, and concrete. Geiger counts provide qualitative knowledge of the variation in the background radiation which may be correlated with the variation in radon counts.

3. Since our Geiger counter is away from the radon site, it may not be highly correlated with readings from the radon sensor. However, we hope to see it can capture the variations caused by changes in the space weather activity and the earth's atmosphere.

4. At the time of writing this thesis, we deployed the Geiger setup for just 8 weeks. We need to collect data over a longer period to verify the ideas in 1 and 3.

The gray wire of the Geiger counter is connected to the Arduino via a white breadboard as shown in Fig. 3.3(B). On the same breadboard, we have a DHT11 sensor for the continuous measurement of temperature and humidity. The 'C' program is uploaded on Arduino which captures values of Geiger counts, temperature, and humidity per minute. these values are collectively called 'Geiger data'.

We aim to store Geiger data continuously in the file. So that we can perform an analysis of this data as and when required. For this purpose, we have connected Arduino with a black Raspberry Pi with a blue-colored USB cable as shown in Fig. 3.3(B). When the entire setup is powered up, we are running the Python program on Raspberry Pi. This program receives serial output from Arduino every minute and performs the following operations:

1. Parsing of string values of serial output into appropriate formats. For example, Geiger counts are parsed into integer format while other parameters such as temperature and humidity are parsed into float format.

2. Creating timestamp at that time.

3. Combining Geiger counts, temperature, humidity, and timestamp as data row and write in the storage file.

In Fig. 3.2, we can see that there is a box shown below the node grid. In that box, we have placed the Geiger counter(denoted by yellow color) and radon sensor(denoted by red color) close to each other. We can see in Fig. 3.3(C), the same Geiger counter setup inside a closed box. The Geiger counter, radon sensor near it, and all the sensor nests are running all the time. In section 3.4, we will perform data analysis of Geiger and radon data measurements and understand various correlations.

3.3 Geoscientific Analysis of Soil

The geoscience research team in OpenRadonLab performs Geoscientic analysis which consists of theoretical modeling based on physical, chemical, and environmental parameters of soil samples collected from the deployment site. This analysis is very important for our simulation. We can understand many soil properties and implement them in the simulation to make it more realistic.

As per the online report of USDA if the mean annual temperature is around 60° F and the mean annual precipitation is 45 inches then the type of soil series at that location

should be of type *Appling*. As per the data available online, the mean annual temperature of Atlanta is 61° F, and the mean annual precipitation is 47.5 inches. USDA has declared the location of Georgia as Appling.

For this purpose, the soil core is extracted from Stone Mountain Park for analysis(shown in 3.4). As seen in chapter 2, parameters like bulk density, permeability, soil grain size, and porosity are very important to understand soil characteristics and ultimately radon flux variation. These parameters are measured and analyzed in the laboratory. Following our soil studies, We have identified that the soil series at our deployment site(Stone Mountain, GA, USA) is Appling series [2]. In chapter 4, we will utilize the knowledge about soil series.

Figure 3.4: Soil core extracted from Stone Mountain, GA, USA.

3.4 Analysis of Geiger and Radon Data

In this section, we perform an analysis of Geiger and radon data collected at Stone Mountain. In this analysis, the correlations between different parameters are studied and also, some important questions are raised which can open different research areas.

We have explained in section 3.2.2, the Geiger setup in detail. In Geiger, data, 3 parameters- temperature, humidity, and Geiger counts along with a timestamp per minute are available. It has been noted that over a minute, there is not much change in the temperature or humidity. However, Geiger counts are highly variable. Hence it is very difficult to study correlation using minute-by-minute data. Hence, the following is taken:

1. The data is re-sampled hourly.

2. For each hour, an average value is calculated for the parameter.

Fig.3.5 shows time series plots of percentage changes in the Geiger counts, temperature, and humidity. Rolling the average over a fixed time interval for Geiger counts shows that Geiger counts have a very good correlation with temperature and humidity. This is aligned with the results of various reference which shows Geiger counts are directly correlated with temperature.

Fig.3.6, Geiger counts are directly proportional to the temperature values with the Pearson correlation coefficient of 0.78. There are outliers present in the data. This is a pretty good correlation since our time series data is not over a long period. A possible reason for the direct correlation could be as temperature increases, the amount of emitted energy (radiation) increases.

Fig.3.7 shows time series variation of Geiger counts and radon counts over approx 2 months. It is important to note that radon data is recorded by sensor 39 in the sensor nest grid. This sensor is located at some distance from the Geiger counter but shows a better correlation (Pearson's $r = 0.31$) compared to other radon sensors. As per reference [5], Geiger counts should show a very good correlation with radon count. We need to record data over a longer period to study variations.

The study of variation of Geiger counts with radon and other environmental parameters may open different research areas. Our simulation is also capable to record gamma particle emission during radon decay. On the other hand, the Geiger counter also detects gamma rays. Therefore, one of the immediate applications of the Geiger counter setup is to study variation and compare the results with the simulation. Geiger counts are also related to space weather activity such as cosmic rays. We should study the variation of Geiger counts and cosmic ray flux in the future.

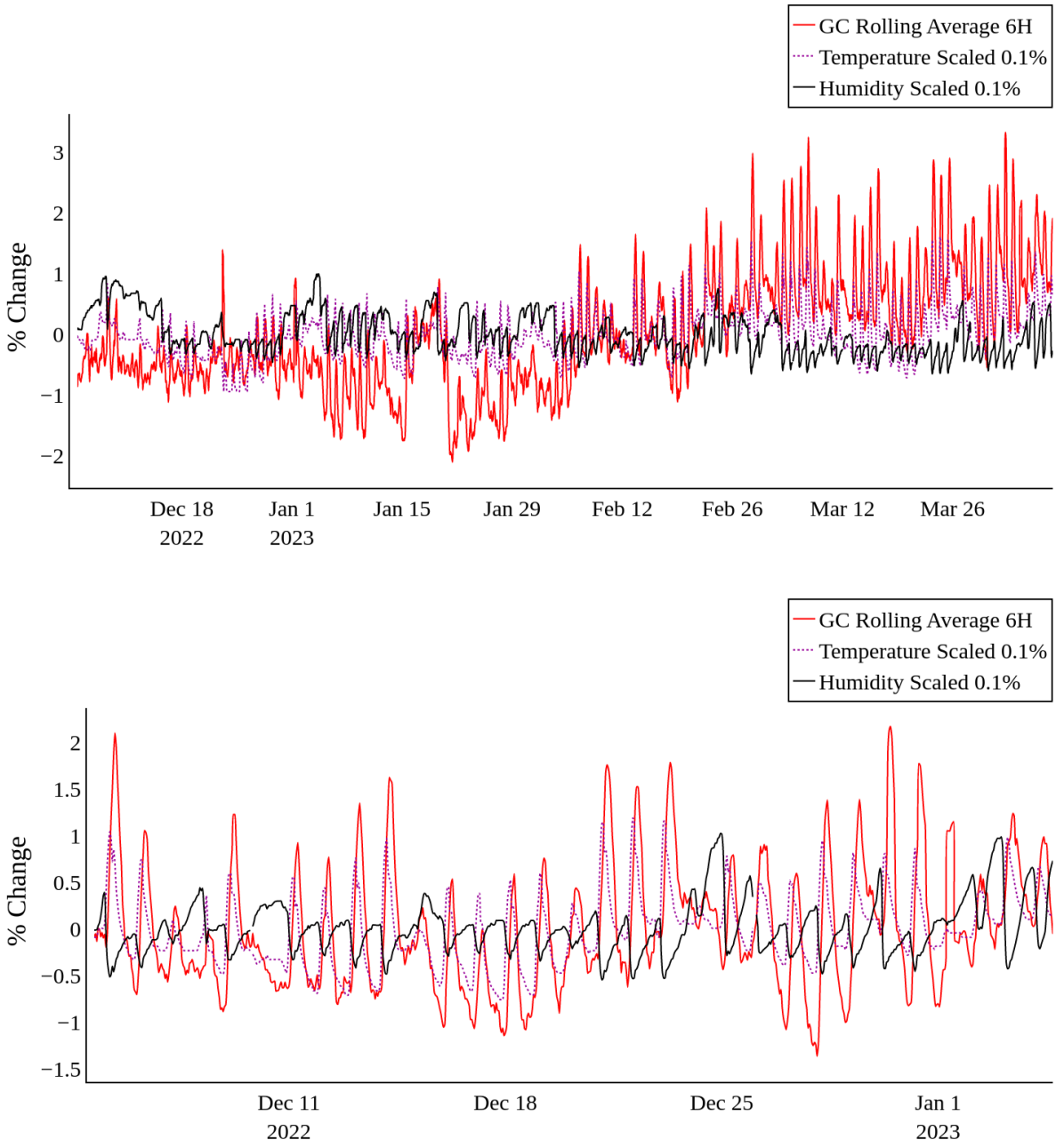

Figure 3.5: Time series plot of percentage change in the Geiger counts(color red), temperature(dotted violet), and humidity(black). Top panel: time series of entire data from December to March. Bottom panel: time series of last month's data to show correlations more clearly.

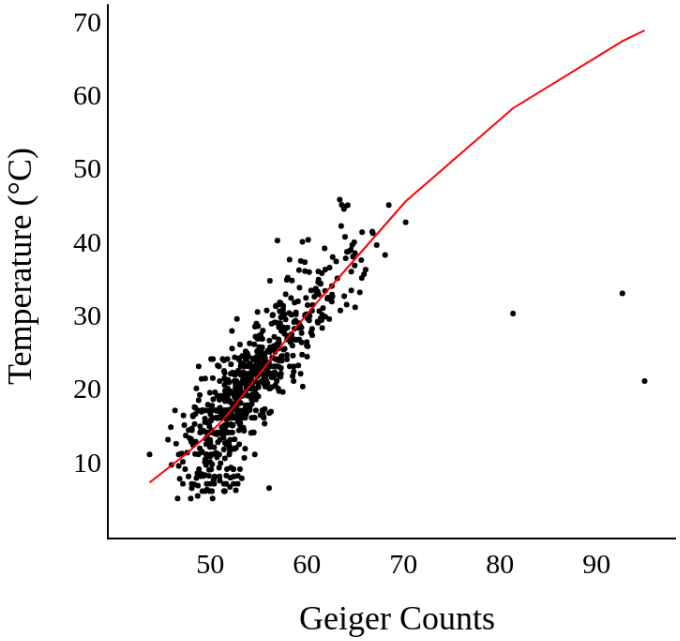

Figure 3.6: Scatter plot shows a correlation between Geiger counts and temperature. Pearson's r = 0.78.

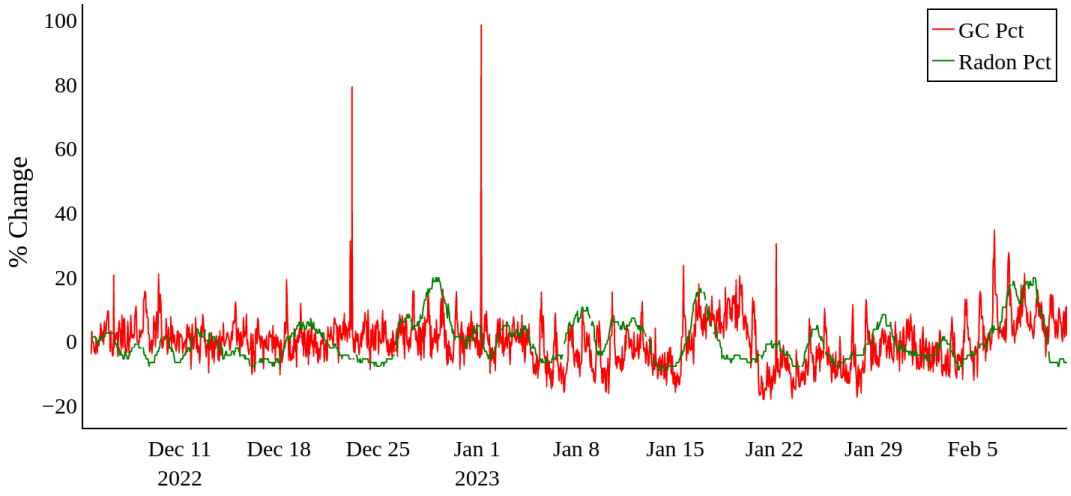

Figure 3.7: Time series plot shows the variation of percentage change in the Geiger counts(color red), and radon flux(color green).

4 RADON PROPAGATION STUDY SIMULATION

4.1 Geant4 Simulation Package

The radon propagation study (RPS) simulation is based on the Geant4 package. It is designed to model soil layers and properties of soil at a microscopic level to understand the effects on radon propagation. Geant4, GEometry, And Tracking is a toolkit for simulating the passage of particles through matter. It is developed by CERN using C++ which is an object-oriented programming language. Participating groups for the development of Geant4 include experimental teams and collaborations, laboratories, and national institutes [17].

The Geant4 simulation package is based on Monte Carlo methods. It offers a wide range of functionalities for simulation development such as geometry, materials, particle interaction with matter, physics models, tracking, and visualization. Physics lists in Geant4 provide a variety of physics processes such as electromagnetic, radioactive decay, and hadronic processes. These processes are applied to a particle that is transporting through the matter. Physics processes can be applied over a wide energy range starting from 0 eV to several TeV energy. We gradually improved our knowledge of physical processes in RPS simulation. We will discuss it in detail in subsequent sections.

We have followed a step-by-step process for developing an RPS simulation. During that period, we faced many challenges in untangling and solving fundamental problems. Therefore, we have taken reference from available literature to logically solve problems. The following sections detail the gradual development.

4.2 Initial Development of RPS Simulation

4.2.1 RPS simulation setup

Geant4 includes a *Geometry* module that provides the capability to describe geometrical structures. Using these geometrical structures we create our detector geometry in simulation. The detector geometry in Geant4 is made of several volumes. The largest volume is *World* volume. All other volumes created are placed inside the world volume. You can consider world volume as the boundary of simulation. Each volume in the geometry has a shape. This shape is described by a concept called *Solid*. The solids define our three-dimensional detector geometry. Geant4 offers a variety of solids, including a cubes, a cylinder, a sphere, a trapezoid, and many others.

To begin our simulation development, we considered soil layers. In section 3.3 we have discussed that the soil series identified in Stone Mountain Park is the Appling series.

Table 4.1: Soil horizons in Appling soil series from reference [2]

Soil horizon	**Depth**
Ap	0-6 inches
E	6-9 inches
B (combining all B horizons)	9-53 inches
C	53-80 inches
Rock	below 80 inches

Keeping in mind that we have 5 different simplified soil horizons in the soil series, we started with spherical geometry. The size of every soil horizon equals the radius of the sphere. We converted depths from Table 4.1 to centimeters and set the radii of five soil horizons as follows:

Table 4.2: Depth of each soil layer (in cm) in RPS simulation

Soil horizon	**Depth**
R5	100 inches (254 cm)
R4	94 inches (238.76 cm)
R3	91 inches (231.14 cm)
R2	47 inches (119.38 cm)
R1	20 inches (50.8 cm)

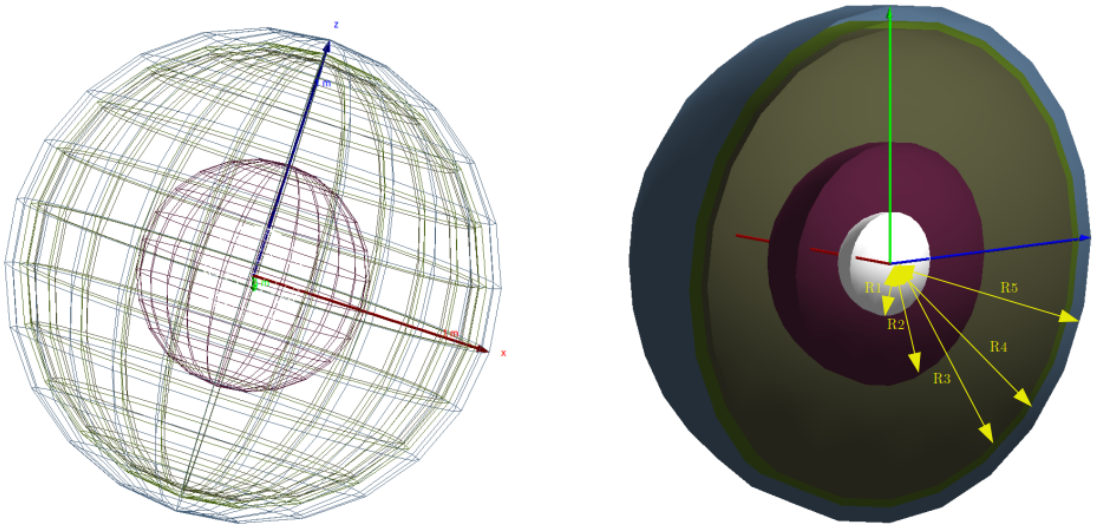

(A) (B)

Figure 4.1: (A) Outer view of soil layers with a total radius of 254 cm. (B) Cross-section view of soil horizons with 5 concentric soil horizons each with a different radius.

After creating a geometry of our soil horizons, we started to explore the chemical composition of soil horizons and how we can specify them in the simulation. In Geant4 G4Element class provides the ability to describe the properties of elements such as atomic number,

atomic mass number, mass per mole, etc. Using G4Element we can create fundamental elements such as H, O, N, C, Ra, Rn, Si, Mg, Al, etc. in simulation. The G4Material class utilizes the elements created by G4Element class to create materials. It describes the properties of the material in geometry such as density, pressure, temperature, etc. So using the G4Material class, we created chemical compounds that can predominantly exist in the soil such as SiO_2, Al_2O_3, Fe_2O_3, CaO, MgO, TiO_2, H_2O, and organic matter.

From section 2.2.1 and section 2.2.4, we know that moisture content affects radon emanation and diffusion. Hence, to make soil horizons more realistic we added varying moisture (H2O content) in each soil horizon. Every soil horizon has SiO2, Al2O3, Fe2O3, CaO, MgO, TiO2, and organic matter in common but different H2O content. Table 4.3 shows the moisture content in each soil horizon:

Table 4.3: Moisture level in each soil horizon in RPS simulation.

Soil horizon	**Moisture content (H_2O %)**
Layer 1 (radius=R5)	0%
Layer 2 (radius=R4)	10%
Layer 3 (radius=R3)	20%
Layer 4 (radius=R2)	30%
Layer 5 (radius=R1)	40%

4.2.2 Introduction to physics processes

The physics process defines how particle traveling through geometry interacts with the material. All physics processes in Geant4 implement the G4VProcess interface to define properties and methods of particular physics processes. There are mainly seven types of processes in Geant4. They are transportation, optical, decay, electromagnetic, hadronic, parameterization, and photoelectron-hadron. There are application-specific physics processes

as well which extend the properties of these physics processes. Users can import any type of process they need and assign it to the particle to use in simulation.

When we combine multiple physics processes into a consistent set, it is called a 'Physics List'. Users can either create their physics list using the physics processes available in Geant4 or use the built-in physics list in simulation. Depending upon the type of simulation, the user can choose one of the two ways. If users have a correct understanding of simulation physics, they can create a custom physics list using the physics processes they want. But this can produce inaccurate results if used physics processes do not apply to a scenario of simulation.

Since, in the beginning, our knowledge of physics required in the simulation was limited, we built our physics list with the following physics processes:

1. *G4EmStandardPhysics* performs pair production and multiple scattering.
2. *G4DecayPhysics* performs decay of unstable particles such as muons, pion, and kaon.
3. *G4Radioactivation* simulates the decay of radioactive isotopes.
4. *G4IonPhysics* performs ionization, multiple scattering, energy loss, nuclear reactions, and other interactions between ions and matter.
5. *G4EmExtraPhysics* provides low-energy interactions which are not included in the standard physics process (*G4EmStandardPhysics*) such as low-energy Compton scattering and pair production.
6. *G4IonElasticPhysics* provides a physics model for the elastic scattering of ions.

It is also important to note that the *G4Transportation* process is included by default in Geant4. It is the main process class responsible for the transport of particles through matter. Since the primary particle in our simulation is radon, a radioactive element, *G4RadioactiveDecay* is the most important process for us. Since we are studying radon propagation we need to understand *G4Transportation* in detail as well. In the next sections, we will discuss these two processes in detail.

4.2.3 Two-body decay kinematics

Two-body decay is a specific type of particle decay in which a parent particle decays into exactly two daughter particles. The kinematics of a two-body decay describes the properties of the parent particle, the daughter particles, and the distribution of their energies and momenta. We used mathematical calculations of Two-body decay kinematics to verify the recoil energy of radon emanation [18].

The alpha decay of radium ${}^{226}_{88}\mathrm{Ra} \longrightarrow {}^{222}_{86}\mathrm{Rn} + {}^{4}_{2}\mathrm{He}$ is of type $\wedge \rightarrow p\pi$ decay. Let $m_{\wedge}$, m_p, and m_π be the mass of ${}^{226}_{88}\mathrm{Ra}$, ${}^{222}_{86}\mathrm{Rn}$, and ${}^{4}_{2}\mathrm{He}(\alpha$ particle) respectively. Given that $m_{\wedge} = 226.02540\ amu$, $m_p = 222.01757\ amu$, $m_\pi = 4.00260\ amu$.

$$E_p = \frac{m_{\wedge}^2 + m_p^2 - m_\pi^2}{2m_{\wedge}} = 222.0176626\ amu,$$

$$P_p = \sqrt{E_p^2 - m_p^2} = 0.202774906\ amu,$$

$$P_p = 0.202774906 \text{ x } 931.49 = 188.8827972 \text{ MeV}.$$

We can directly use the calculated momenta of radon 188.8827972 MeV in the RPS simulation which it internally converts into kinetic energy of 86.28 KeV.

4.2.4 Generation of primary events

After creating the geometry, adding materials, and specifying the required physics processes, we need to specify how a primary event should be generated. In Geant4, *G4VUserPrimaryGeneratorAction* concrete class provides properties and methods to specify a primary event. some important points to keep in mind regarding primary events in Geant4 are: 1) Primary event allows specifying properties primary particle to start the simulation, 2) User can start a run with n several primary events, and 3) User should specify vari-

ous properties of a particle such as energy, initial position in geometry, charge, momentum, momentum direction, atomic number, and atomic mass number.

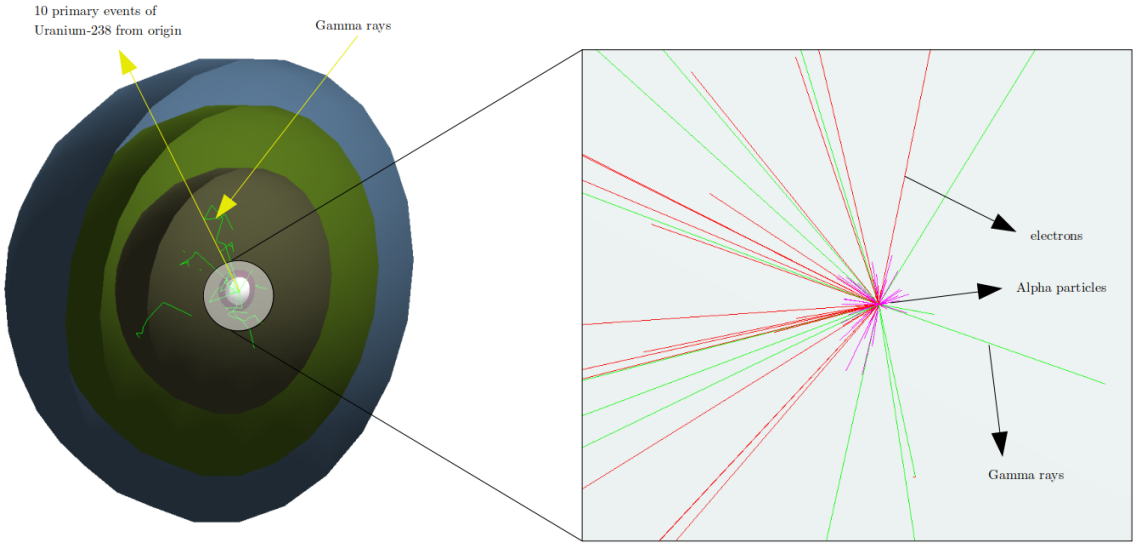

Figure 4.2: (A) 10 events with primary particle ^{238}U from the center position of geometry. (B) Zoom-in view of (A) which shows other generated particles. Gamma rays (color green) are highly penetrating radiation that travels through various hard materials in soil horizons. The simulation also generates electrons and other generic ions which are part of the radioactive decay series of uranium.

We started our development with a primary particle as ^{238}U which sits at rest. i.e. initial kinetic energy in the primary event is equal to zero. This is because of the following reasons.

First, as shown in Fig. 1.1, radon is one of the decay products in ^{238}U decay chain. Also, Uranium sits at rest deep in the bedrock and eventually undergoes decay to produce all other decay products including ^{222}Rn. Second, in the future, through our simulation, we plan to get uranium concentration in the soil at Stone Mountain Park. Hence, it will be easier for

us to compare our results. Third, we wanted to see how radioactive decay is processed with our initial setup of physics processes and materials.

At each step of development, we need to analyze the data generated at the end of each run of the simulation. This helps us to verify the correctness of the simulation. This analysis is performed using ROOT framework [19]. ROOT is a data analysis framework based on C++ developed by CERN.

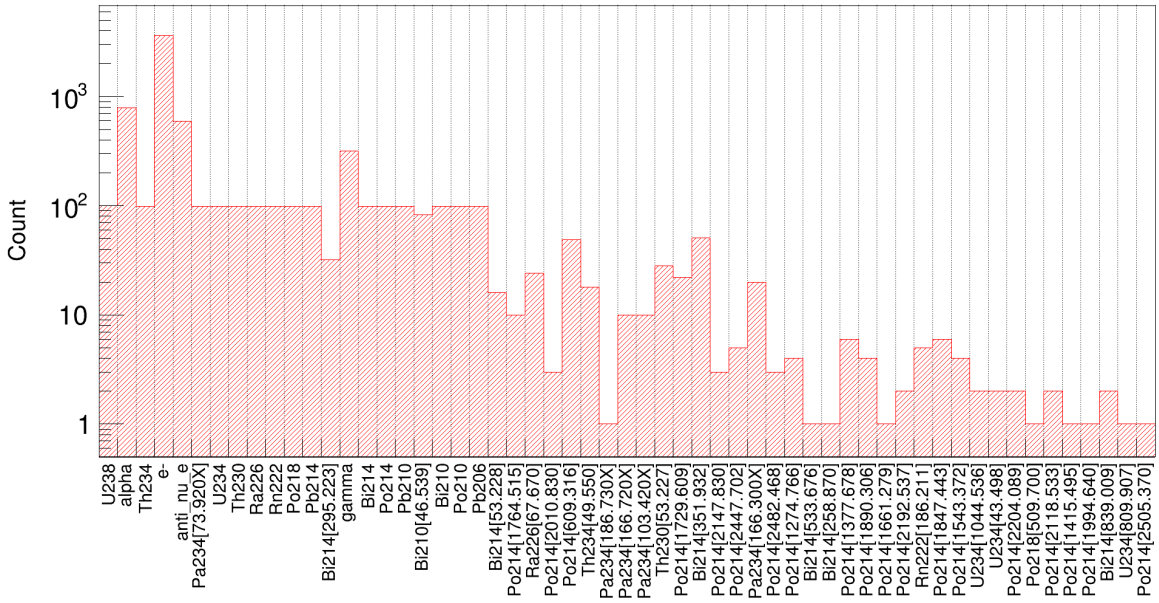

Figure 4.3: Decay products generated in simulation. The simulation started with 100 primary events of ^{238}U at rest from the center in spherical soil horizon geometry and soil materials specified in Section 4.2.1.

Next, with the same setup, we started a run of 100 events of ^{238}U. We analyzed the results for each layer of soil horizon. We found out various decay products get generated throughout the geometry. Fig.4.3 shows various decay products generated in layer 5. We can see that count of ^{238}U is 100 which is equal to the number of primary events.

It is also important to note that some intermediate decay particles are also recorded during a run of the simulation like Pa234[166.300X], Pa234[166.300X], and Pa234[73.920X]. These particles are isotopes of ^{234}Pa (protactinium). This is the notation used by Geant4

while processing radioactive decay. Exploring the hows and whys of these isotopes is not in the scope of our research as this is automatically handled by Geant4 software. Similar kinds of results can be generated by Geant4 for other elements as well.

In the next section 4.2.5, we will perform a more detailed analysis of recorded data and discuss a few problems and challenges in simulation development as we go forward in our research.

4.2.5 Initial data analysis in RPS simulation

The main goal of the simulation is to study radon propagation through the soil and measure flux at the defined surface from a particular depth. We want to study how far radon is traveled if we start with the primary particle as uranium at rest. To study how radon travels through soil horizons, we recorded (x,y,z) coordinates in each step.

To verify our recorded data, we started by analyzing gamma rays. In Fig.4.2, It is observed that gamma rays are traveling through all the soil horizons. This is because gamma rays are highly penetrating radiation. Fig.4.4 shows the distribution of distance covered by gamma rays as expected. Few gamma rays traveled up to 350 cm distance (up to the simulation boundary). Distances are calculated using $\sqrt{x^2 + y^2 + z^2}$ from origin (0,0,0).

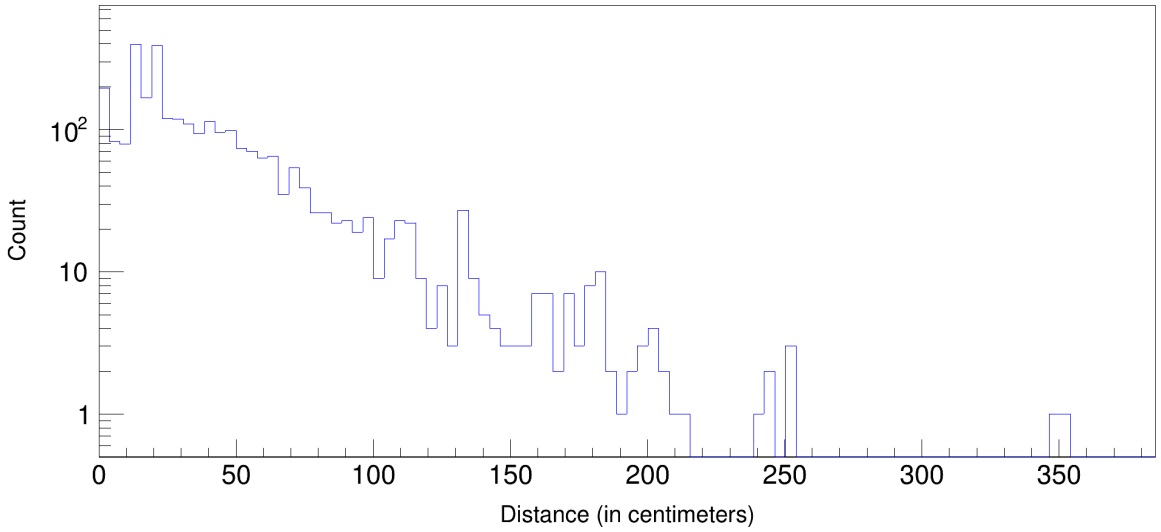

Figure 4.4: Count of gamma rays traveled up to specific distances when soil horizons are composed of various chemical elements.

We observed that with our current setup, radon particles traveled up to an extremely short distance of approximately 7 x 10^{-6} micrometers from the origin as shown in Fig.4.5.

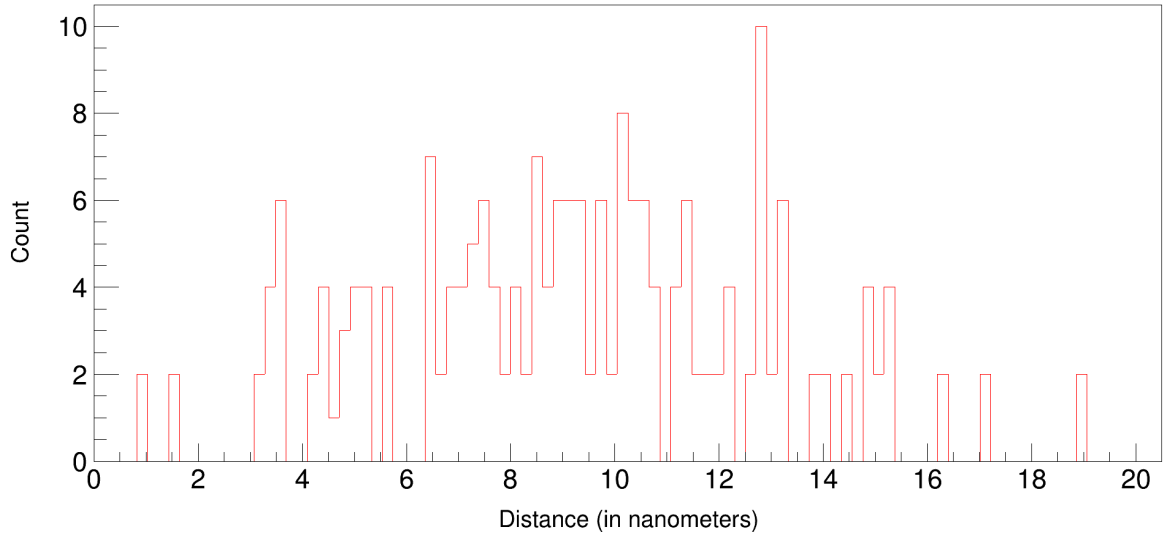

Figure 4.5: Count of radon particles traveled up to specific distances when soil horizons are composed of various chemical elements.

Since it was a very short distance, we further analyzed the distance traveled by radon particles in water and air. As shown in Fig.4.6 and Fig.4.7, radon particles travel upto 60 nanometers in water and upto 60 micrometers in air.

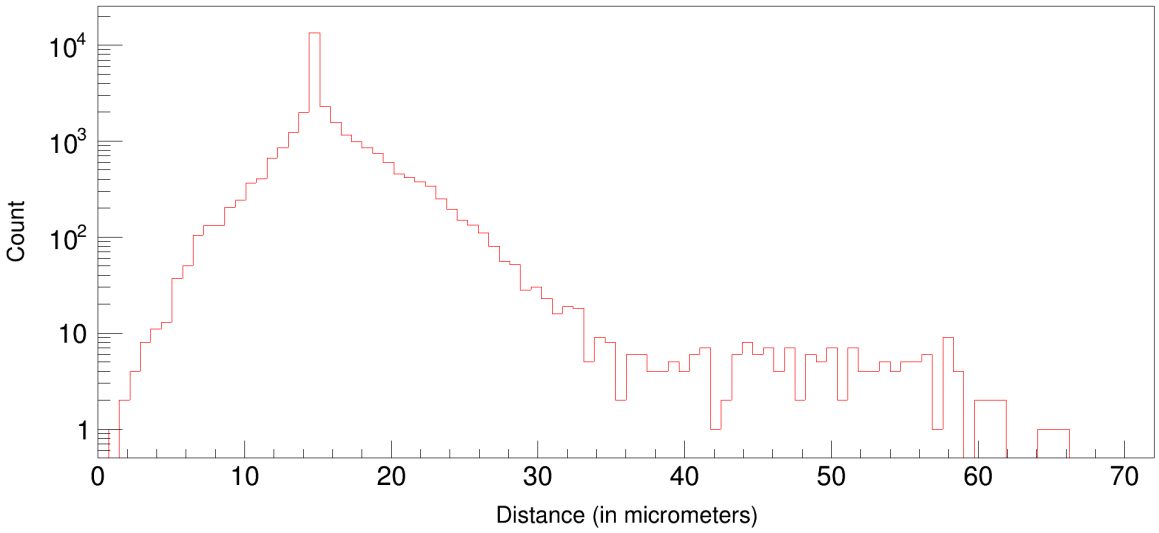

Figure 4.6: Count of radon particles traveled up to specific distances in air medium.

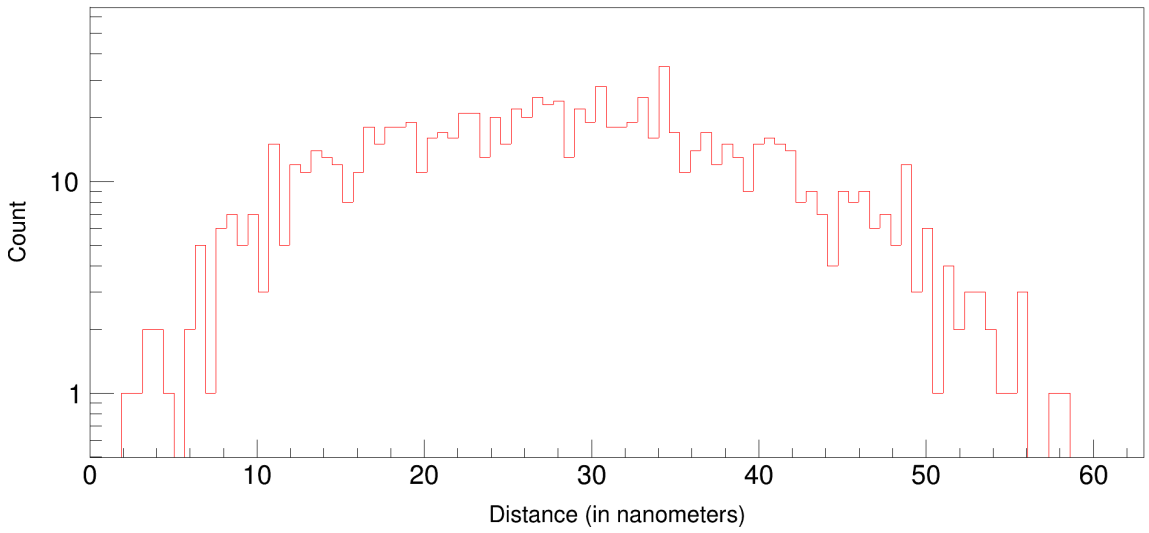

Figure 4.7: Count of radon particles traveled up to specific distances in water medium.

The observation distances traveled by radon are important for us because we aim to study propagation. It is clear radon particles travel a much better distance through water

and air than the solid chemical composition of Layer 1. Since layer 1 does not have moisture content and free space, radon particles are unable to move.

Table 4.4: Recoil ranges of radon in various mediums calculated using the SRIM software package. Data were taken from IAEA's (International Atomic Energy Agency) 'Measurement and Calculation of Radon Releases from NORM Residues' report in 2013 [3].

Medium	**Density (gm/cm^3)**	**Range (nm)**
Air	1.58 x 10^{-3}	53,000
Water	1.00	77

We can have a look at Table 4.4 which shows recoil ranges calculated using the SRIM software package which is used to study 'interactions of ions with the matter'. The distance values recorded by the Geant4 simulation and SRIM package are not the same but qualitatively in a similar range of nanometers and micrometers for water and air mediums respectively.

4.3 Radon Emanation Study

4.3.1 Introduction

For the development of RPS simulation, it is important to study radon emanation. In Chapter 2 Fig.2.3 in and stage 2 in Fig.2.1 show the process of radon emanation in detail. Furthermore, Section 2.2 details the effects of various parameters on radon emanation.

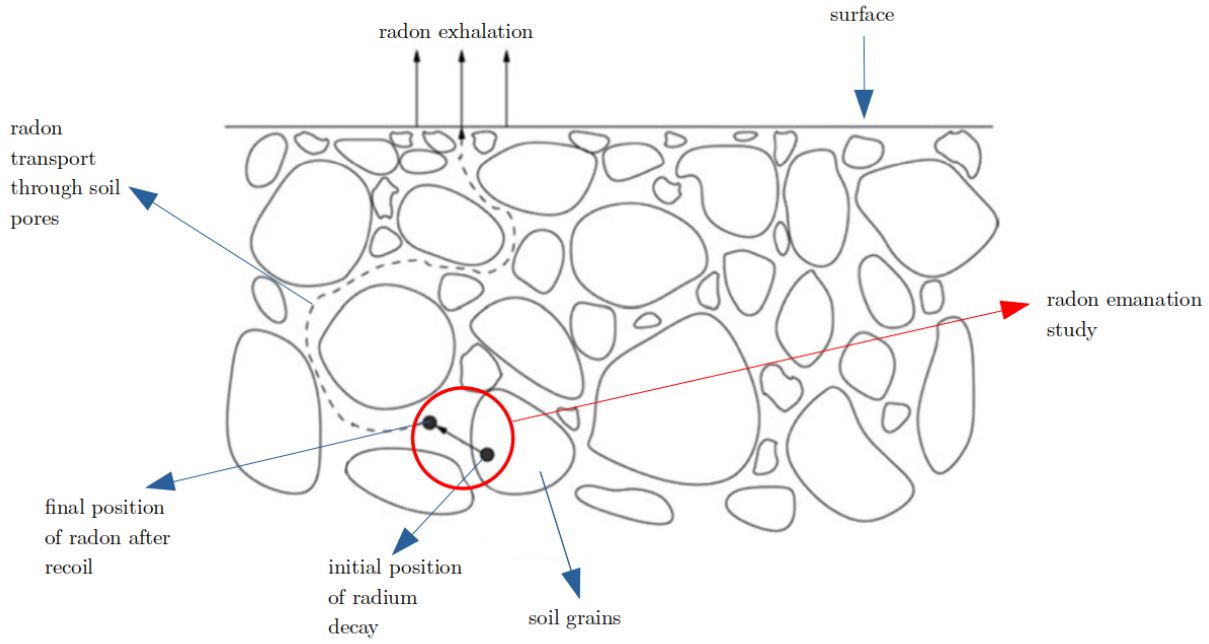

Figure 4.8: Schematic representation of overall radon transport from soil grain to air. The red circle indicates the radon emanation from grain and radon becomes available in pore space. The dotted line indicates the radon transport through the air.

As shown in Fig.4.8, radon emanation is an important part of its transport. Radon emanation is an important factor to understand radon flux variation because if radon emanation is more, more radon may enter the soil pores and get transported to the atmosphere and vice-versa. Hence, modeling radon emanation in RPS simulation is important.

The particle size, shape, and location of ^{226}Ra determine how radon can escape into interstitial pores [5]. In our simulation, we are assuming that the sphericity of the soil grain is 1, and radium is distributed uniformly in the soil grain.

4.3.2 Simulation setup

Since we know how radon travels through different mediums such as air and water. We updated our simulation with the modeling of a single soil grain of size 100 nm. For this setup, the approximate chemical composition of soil grain is defined which should be updated as per requirement in the future. For the current setup, we used a general chemical composition consisting of chemical compounds such as SiO_2, Al_{2O3}, MgO, CaO, and Organic matter following the references [20, 21] and general information available on the web. This chemical composition will be updated in the future when we complete soil analysis at Stone Mountain.

We use the primary particle as radon with an energy of 86 KeV. Let R be the maximum distance traveled by radon in the material (measured in nanometers). Only radon atoms present in range R (0-40 nanometers depending on material) from the surface of the grain can escape the grain. This range R is called recoil range [22] and it is material dependent. After multiple rounds of running a simulation, It is observed that the recoil range R of radon in our simulation is 17 nm. Any radon particle below the depth of 17 nm from the surface will not escape the soil. To study radon emanation, we need to start our simulation by placing radon atoms uniformly in recoil range R. Fig.4.9 shows the simulation setup.

It is important to note that it is not guaranteed that all the radon particles present in range R will escape the grain. Because the emanation also depends on the direction of the recoil. The average probability of radon formed at depth $x \leq R$ escaping from grain is equal to 25% [22]. To conclude, radon emanation is a very random phenomenon.

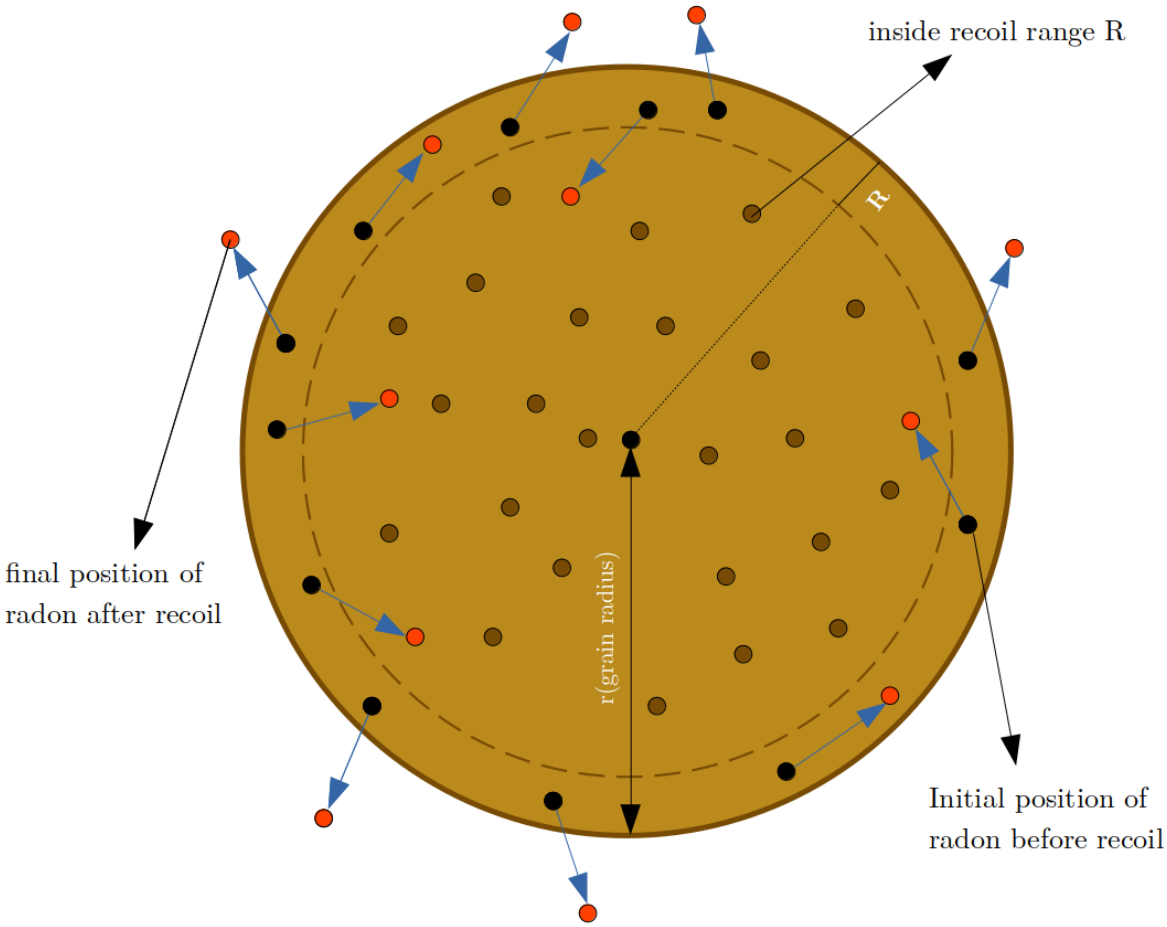

Figure 4.9: Simulation setup of single soil grain with the size of 100 nm and recoil range R is observed to be 17 nm. The radon atoms generated in recoil range R (color black) have the probability to escape the soil grain. The spherical annulus R represents the volume inside which radon particles are located. The initial position before recoil and final position after recoil is denoted with black and white circles respectively. The radon atoms produced below the dotted line will not escape the grain [5].

Since the simulation setup is complete. different parameters influence the radon flux variation in simulation. The following parameters have an impact on radon emanation: 1) moisture content, 2) temperature, and 3) Fe/Mn content and pH in the soil.

Since moisture content has the most significant impact on radon emanation [1, 6], we study the effect of moisture content on radon emanation through our simulation. This will help us to verify the correctness of the simulation and conduct a detailed study about the influence of moisture content on radon emanation.

4.3.3 Effect of moisture content on radon emanation in single soil grain

The Radon emanation coefficient is defined as the fraction of radon that escaped from the soil grain and the total radon produced in the soil grain. As discussed in the previous section, the radon emanation coefficient is material specific. Some methods to calculate the radon emanation coefficient are Gamma-ray spectrometry and the Accumulation method. It is worth noting that measured emanation coefficients are considerably higher than calculated by theoretical or physical models [1].

In section 2.2 we discussed the effect of moisture content on radon emanation. To put it simply, as moisture content increases, radon emanation increases. Fig. 4.10 shows a plot of radon escaped from soil grain (%) vs moisture content based on data recorded by simulation.

Starting from 0%, we increased moisture gradually by 10% in each run. Each run consists of 10,000 events. We increased moisture up to 100%. It is observed that upon increasing the moisture level, radon emanation increases. This is because radon emanation is more if the source material is moist or wet rather than dry [5].

It is crucial to keep in mind that different references may employ different chemical compositions, experimental setups, and assumptions. Our setup and chemical composition are also different from other references. Therefore, even though the results may not be the same as those in other references' graphs, they should be qualitatively similar and comparable.

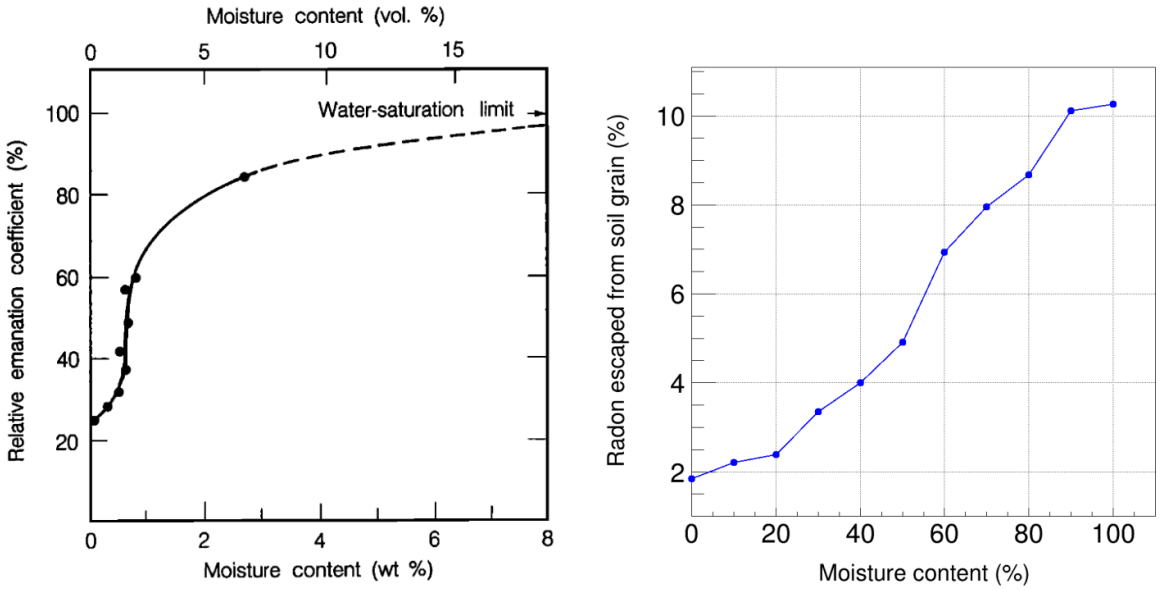

(A) (B)

Figure 4.10: (A) Effect of moisture content on relative radon emanation coefficient for a sample of uranium mill tailings [1]. (B) Dependence of radon emanation on moisture content with grain size 100 nm for 10,000 events in each moisture level. Similar correlations are observed in [1,6,7], and multiple papers which show moisture content is directly proportional to radon emanation.

Fig.4.10 shows that the results of our simulation are qualitatively similar to the references. While the single soil grain model is good for basic study. In reality, we will have multiple grains in the soil samples. Hence, it is important to extend the simulation setup from single grain to multiple grains. This will help us to understand the influence of moisture content on radon emanation in more detail.

4.3.4 Effect of moisture content on radon emanation with multi-grain setup

In this section, we are interested in understanding the effect of grain size on radon emanation. In the ideal case, in a single grain model, when the shape of the grain is perfectly spherical and radium content is uniformly distributed throughout the volume of the grain.

If we assume that radium content increase with increased grain size, radon emanation is directly proportional to grain size [8].

But in reality, many studies have been conducted to understand the dependence of radon emanation on particle size. Experimental results on the effect of grain size have been inconsistent. Reference [23] mentioned that particle diameter had no measurable effect on radon emanation while reference [6] mentioned that small-size grains(<0.1mm) have more radon emanation than large-size grains and large size grains reaches saturation points faster. Reference [8] concluded that radon emanation increases with an increase in grain size when located uniformly at depth R. Reference [24] concluded that in simple cubic structure (SCS) when radon particles are located uniformly at depth R, radon emanation increases with increase in grain size. In a face-centered cubic structure (FCCS), when radon particles are uniformly located in soil grain, radon emanation decreases with an increase in soil grain.

In short effect of grain size on radon emanation can be only determined if we know the distribution of radium and the amount of radium content in the soil. For our simulation, since we have already assumed radium is uniformly located in recoil range R, we will proceed with the existing setup.

We updated our simulation setup from one soil grain to multiple soil grains. Fig.4.11 details the updated simulation setup. This simulation setup follows principles mentioned in [8]. The size of all grains is equal and the chemical composition of all grains is the same. We are starting our simulation only from the central grain (color blue).

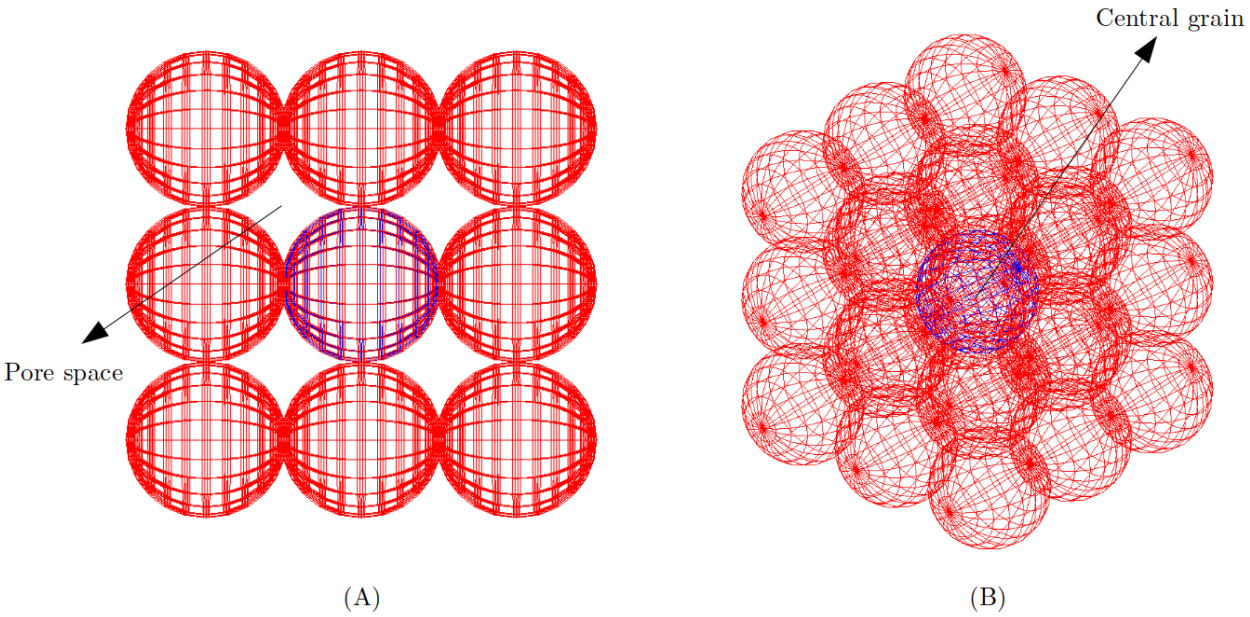

Figure 4.11: Updated simulation setup with multiple soil grains. (A) Top view: the gap between grains acts as a pore gap. (B) Side view: blue-colored grain is the central grain for primary events generation. Red-colored grains are surrounding grains covering the central grain. The setup is identical to the simple cubic structure(SCS) mentioned in reference [8].

If a radon atom escapes from the grain and enters into the neighboring grain, it is not called radon emanation. It is important to understand how moisture content influences radon emanation at the microscopic level.

To understand the influence of moisture content on radon emanation, the grain size is set to 100 nm, and the moisture level throughout the geometry (moisture in grain and moisture in pore space) is set to zero.

Fig.4.12 shows results after simulating 10,000 events. We observed that: 1) many radon particles escape from the soil grain and get embedded in the neighboring grain, and 2) the count of radon embedded in the surrounding grain is greater than the count of radon that comes to rest in the pore space.

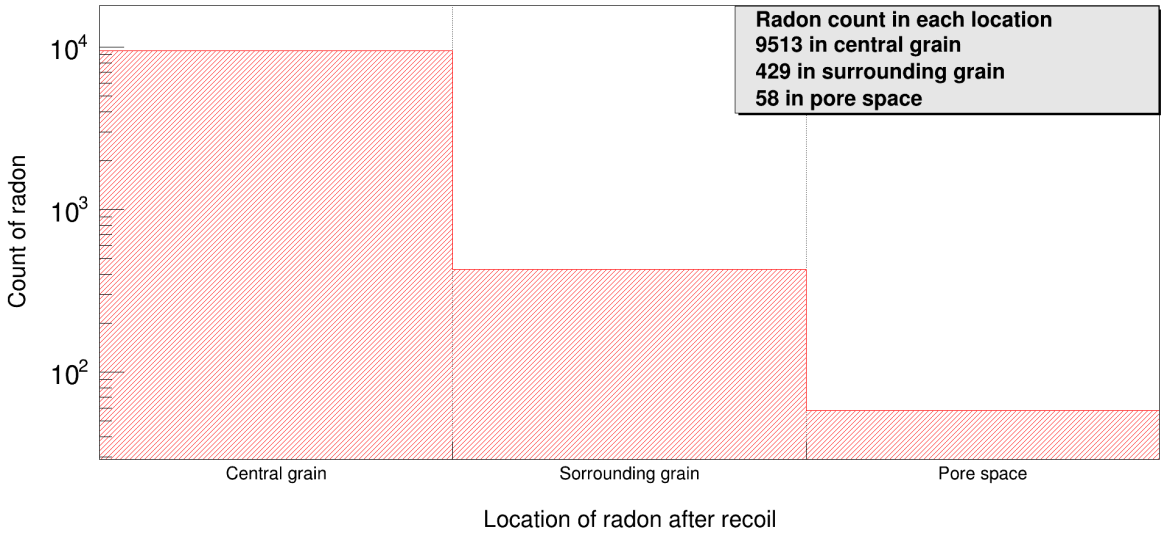

Figure 4.12: Counts of radon particles at different locations after recoil. Grain size is set to 100 nm, number of events is set to 10,000, and moisture level is set to 0.

After observing a very low count of radon in pore space, we gradually increased the moisture level. Fig.4.13 shows the count distribution of radon in pore spaces and surrounding grains when the moisture level is increased gradually.

It is observed that when the moisture level is gradually increased, the count of radon in the surrounding grains (color Magenta) decreases, and the count of radon in pore space (color Blue) increases. Thus radon emanation increases.

This is because of increased moisture levels. Water content terminates the recoil of radon particles. Therefore as the moisture level is increased, the water content can terminate the recoil of radon particles more effectively. Hence, more radon particles can come to rest in the sweet spot i.e. pore space. radon emanation (color blue) is increased as shown in Fig.4.13. So we can conclude that moisture content influences radon emanation in two ways:

1. It makes the soil grain moist which helps the radon to escape from the soil grain.

2. When radon escapes the soil grain, it terminates the recoil of radon which increases the probability of radon coming to rest at the pore space.

This phenomenon is perfectly aligned with results from references [6, 8].

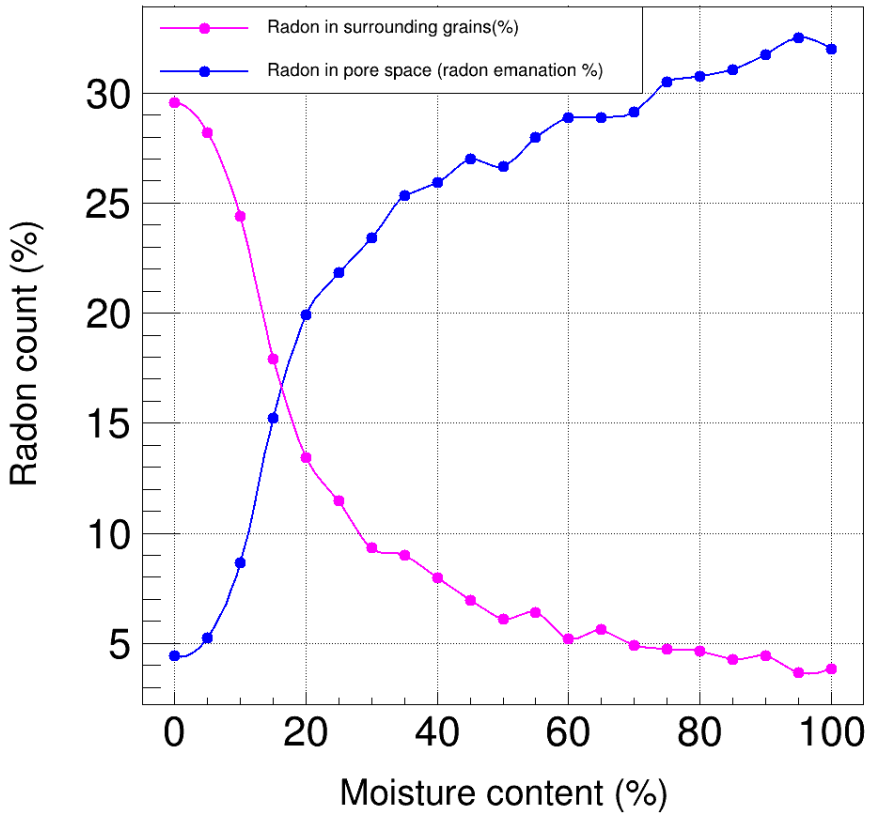

Figure 4.13: Radon counts at two different locations in the soil grain of size 100 nm: 1) Magenta color corresponds to radon count in surrounding grains and 2) Blue color corresponds to radon count in interstitial pore space.

After determining how moisture content affects radon emission, the simulation study is expanded to determine how grain size affects radon flux. We are interested in the measurement of the radon emanation coefficient as a function of moisture content and grain size.

For this study, three different grain sizes are taken- 100 nm, 200 nm, and 300 nm. The simulation is run separately for each grain size with a gradual increase in moisture level.

Fig.4.14 (Top panel) shows the radon emanation coefficient as a function of moisture content and grain size measured through simulation. Important findings from the results include the following:

1. In each grain size, radon emanation increases as moisture content increases. The results also indicate that the radon emanation coefficient in dry soil is relatively low as compared to moist soil. This is already explained with Fig.4.12.

2. Rate of increase of radon emanation is different in different grain sizes. It is observed that as grain size increases radon emanation decreases. This observation perfectly aligns with references [6,8]. In reality, Small particles have more surface area. Therefore radon particles can focus near the grain surface as compared to samples with large particles. Therefore, it is observed that the radon emanation coefficient is more in small grain sizes. In our simulation, as grain size increases, the probability of radon escaping from the grain decreases.

3. Fig.4.14 (Bottom panel) shows that at higher moisture content saturation is observed for the radon emanation coefficient. This is because, at higher moisture content, very few radon particles enter into adjacent soil grains. Hence radon emanation coefficient remains constant after a particular point even though moisture content is increased. In our simulation, we observe small saturation after 85%. We may find better results that match with reference [6] in the future.

Fig.4.14 shows the comparison of experimental results mentioned in the reference [6] and simulation results.

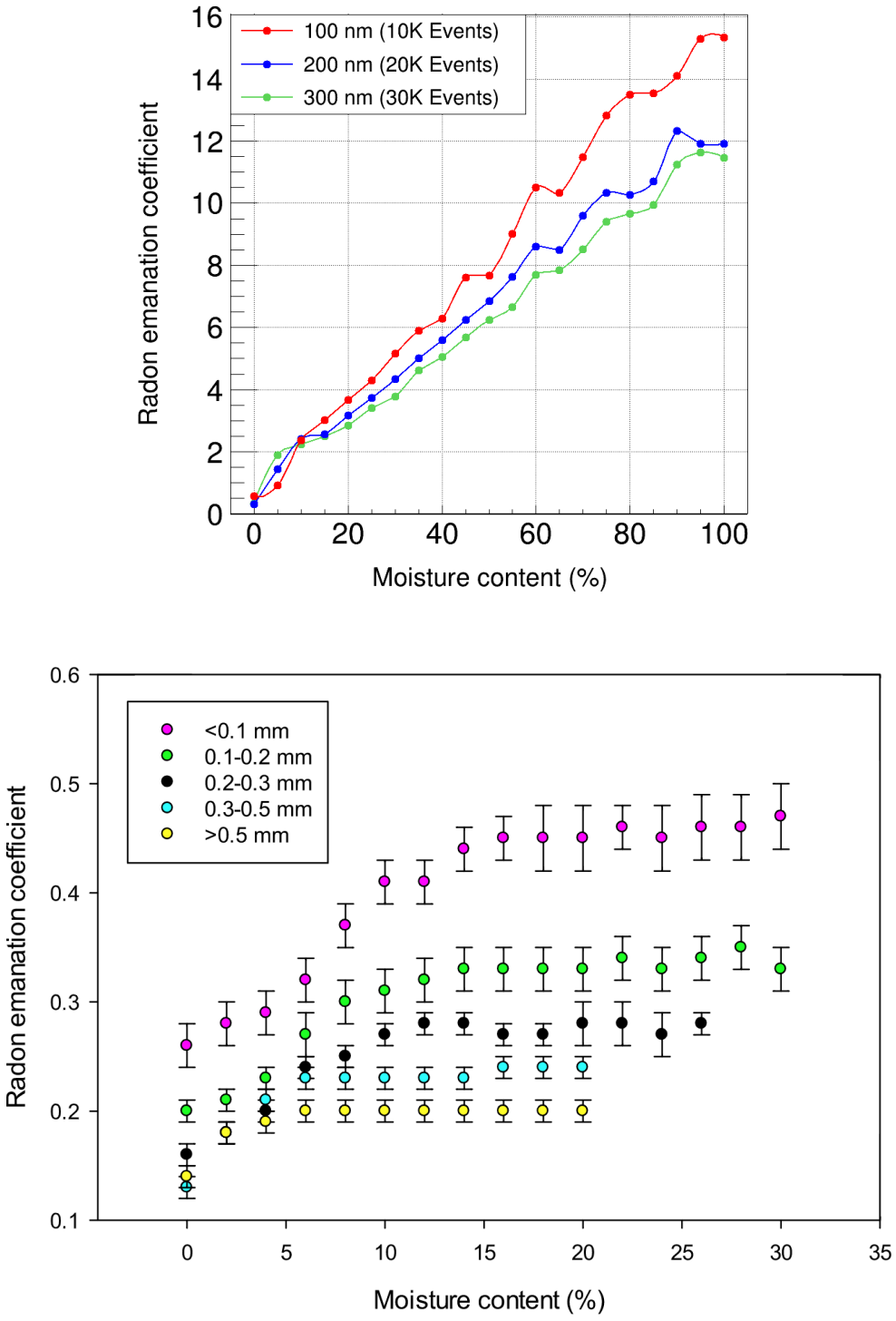

Figure 4.14: Top panel: Dependence of radon emanation on moisture content and grain size based on data recorded by RPS simulation. Bottom panel: Dependence of radon emanation on moisture content and grain size from reference [6].

4.4 Limitations of Geant4 for RPS simulation

In Section 2.2 we have studied that experimental results also showed temperature, Fe/Mn content, and pH shows good correlation with radon emanation.

The high pH and high content of Fe/Mn oxides and Fe/Mn oxyhydroxides precipitates have high radium adsorption capacity. As an effect, more radium grains tend to sorb onto the surface of the grain. This phenomenon increases radon emanation. As of now, no application process in Geant4 simulates adsorption. As a result, the thesis does not examine the effects of these parameters.

We have completed the radon emanation study. But once it enters into pore space, further transport is governed by diffusion or advection process. We have already discussed that Geant4 does not have an applicable physics process to simulate diffusion. Hence, we cannot study radon migration governed by diffusion in Geant4. However, future work includes the development of a separate simulation program to study radon migration through soil assuming the transport is governed by advection.

5 SUMMARY AND OUTLOOK

Although the scientific community has conducted a great deal of research to understand how radon propagates through the soil, the problem to understand radon propagation in the soil through Geant4 has never before been attempted.

A major effort has been made to comprehend various concepts of radon propagation in the soil through scientific literature and implement those concepts for the development of a simulation program, called RPS (Radon Propagation Study) simulation. A significant amount of work was undertaken to develop RPS simulation including (1) a detailed study of scientific literature on radon propagation through the soil; (2) the implementation of proper physics processes and verification of the correctness of simulation; (3) the extensive and flexible simulation output scheme which allows analyzing the radon propagation after radium decay using the advanced data analysis tool - ROOT [19].

Part of this thesis work is to develop an IoT setup with a Geiger counter, Arduino, and Raspberry Pi. This setup has been deployed at Stone Mountain Park, Atlanta and it collects real-time data including Geiger counts and temperature every minute. The importance of this setup includes, but is not limited to:

1. providing real-time data to study patterns of variations of Geiger counts caused by changes in temperature, radon counts, and space weather activity (cosmic rays).

2. providing real-time data that can be used for the combined study of Gamma rays generated in RPS simulation and Geiger counter data collected at Stone Mountain Park, Atlanta, and temperature.

One of the immediate important applications of RPS simulation is to understand key features of radon through the developed Monte Carlo simulation program. RPS simulation allows us to study the effect of moisture content on radon flux variation in different grain sizes. The results of the simulation are qualitatively similar to various published results. It also offers scalability to extend functionalities in the future through object-oriented programming (OOP) features of C++.

Future work includes improvement in radon emanation study by updating the chemical composition of soil grain, grain sizes, and pore-gap lengths. Depending upon the future requirements, the geometry of the simulation can be updated to more complex such as multiple grains with variable size and/or face-centered cubic structure (FCCS). Currently, we have used very small grain sizes in nanometers. But in reality, grain sizes can vary from nanometers to millimeters. Therefore, grain size should be updated as per requirement.

As part of RPS simulation, a separate simulation program is being developed called a radon migration study. This will help us to understand radon migration through soil pores assuming that transport is governed by advection. It uses a custom physics process called the 'DriftPhysics' process which uses the drift velocity of air for radon transport through pore space. This is crucially important for understanding overall radon transport from soil to air.

REFERENCES

[1] W. W. Nazaroff, "Radon transport from soil to air," *Reviews of Geophysics*, vol. 30, no. 2, pp. 137–160, 1992.

[2] U. S. D. of Agriculture, "Appling series," 2005.

[3] P. M. Y. M. M. P. Y. Ishimori, K. Lange, "Technical reports series no. 474, measurement and calculation of radon releases from norm residues," 2005.

[4] D. M. Strong, Kaye P.; Levins, "Teffect of moisture content on radon emanation from uranium ore and tailings," *Health Physics*, vol. 42(1):p 27-32, 1982.

[5] M. Baskaran, *Radon: A Tracer for Atmospheric Studies*, pp. 63–83. Cham: Springer International Publishing, 2016.

[6] H. N. P. Thu, N. V. Thang, and L. C. Hao, "The effects of some soil characteristics on radon emanation and diffusion," *Journal of Environmental Radioactivity*, vol. vol. 216, 2020.

[7] G. J. J. F. e. a. Fournier, F., "Simulation of radon transport through building materials: Influence of the water content on radon exhalation rate.," *Transp Porous Media*, vol. 59, p. 197–214, 2005.

[8] A. Sakoda, K. Hanamoto, Y. Ishimori, T. Kataoka, A. Kawabe, and K. Yamaoka, "First model of the effect of grain size on radon emanation," *Applied Radiation and Isotopes*, vol. 68, no. 6, pp. 1169–1172, 2010.

[9] A. Marefat, A. A. M. Nishar, N. Karve, and A. Ashok, "Openradon lab: Democratizing soil radon modeling and mapping," p. 593–594, 2022.

[10] World Health Organization, *WHO Handbook on Indoor Radon: A Public Health Perspective*. Nonserial Publications Series, World Health Organization, 2009.

[11] J. Lab, "Alpha decay," 2015.

[12] L. C. S. Gundersen, R. R. Schumann, J. K. Otton, R. F. Dubiel, D. E. Owen, and K. A. Dickinson, "Geology of radon in the United States," in *Geologic Controls on Radon*, Geological Society of America, 01 1992.

[13] J. K. Otton, "Geology of radon online report," 2011.

[14] A. Tanner, "Radon migration in the ground: a supplementary review," *Conference on natural radiation environment III*, vol. 12, no. 16, 1980.

[15] S. D. Schery, D. H. Gaeddert, and M. Wilkening, "Factors affecting exhalation of radon from a gravelly sandy loam," *Journal of Geophysical Research*, vol. 89, pp. 7299–7309, 1984.

[16] W. contributors, "Advection," 12 2022.

[17] S. Agostinelli, J. Allison, K. Amako, J. Apostolakis, H. Araujo, P. Arce, M. Asai, D. Axen, S. Banerjee, G. Barrand, F. Behner, L. Bellagamba, J. Boudreau, L. Broglia, A. Brunengo, H. Burkhardt, S. Chauvie, J. Chuma, R. Chytracek, G. Cooperman, G. Cosmo, P. Degtyarenko, A. Dell'Acqua, G. Depaola, D. Dietrich, R. Enami, A. Feliciello, C. Ferguson, H. Fesefeldt, G. Folger, F. Foppiano, A. Forti, S. Garelli, S. Giani, R. Giannitrapani, D. Gibin, J. Gómez Cadenas, I. González, G. Gracia Abril, G. Greeniaus, W. Greiner, V. Grichine, A. Grossheim, S. Guatelli, P. Gumplinger, R. Hamatsu, K. Hashimoto, H. Hasui, A. Heikkinen, A. Howard, V. Ivanchenko, A. Johnson, F. Jones, J. Kallenbach, N. Kanaya, M. Kawabata, Y. Kawabata, M. Kawaguti, S. Kelner, P. Kent, A. Kimura, T. Kodama, R. Kokoulin, M. Kossov, H. Kurashige, E. Lamanna, T. Lampén, V. Lara, V. Lefebure, F. Lei, M. Liendl, W. Lockman, F. Longo, S. Magni, M. Maire, E. Medernach, K. Minamimoto, P. Mora de Freitas, Y. Morita, K. Murakami, M. Nagamatu, R. Nartallo, P. Nieminen, T. Nishimura, K. Ohtsubo, M. Okamura, S. O'Neale, Y. Oohata, K. Paech, J. Perl, A. Pfeiffer, M. Pia, F. Ranjard, A. Rybin, S. Sadilov, E. Di Salvo, G. Santin, T. Sasaki, N. Savvas, Y. Sawada, S. Scherer, S. Sei,

V. Sirotenko, D. Smith, N. Starkov, H. Stoecker, J. Sulkimo, M. Takahata, S. Tanaka, E. Tcherniaev, E. Safai Tehrani, M. Tropeano, P. Truscott, H. Uno, L. Urban, P. Urban, M. Verderi, A. Walkden, W. Wander, H. Weber, J. Wellisch, T. Wenaus, D. Williams, D. Wright, T. Yamada, H. Yoshida, and D. Zschiesche, "Geant4—a simulation toolkit," *Nuclear Instruments and Methods in Physics Research Section A: Accelerators, Spectrometers, Detectors and Associated Equipment*, vol. 506, no. 3, pp. 250–303, 2003.

[18] H.-C. Cheng, "Two-body decay kinematics." Online, 2015. `https://indico.cern.ch/event/391122/contributions/928962/attachments/782786/1073126/twoBodyDecay.pdf`.

[19] R. Brun, F. Rademakers, P. Canal, A. Naumann, O. Couet, L. Moneta, V. Vassilev, S. Linev, D. Piparo, G. GANIS, B. Bellenot, E. Guiraud, G. Amadio, wverkerke, P. Mato, TimurP, M. Tadel, wlav, E. Tejedor, J. Blomer, A. Gheata, S. Hageboeck, S. Roiser, marsupial, S. Wunsch, O. Shadura, A. Bose, CristinaCristescu, X. Valls, and R. Isemann, "root-project/root: v6.18/02," Aug. 2019.

[20] "Gases underground," 2023.

[21] D. of Primary Industries and R. Development, "What is soil organic carbon," 2022.

[22] D. Bossus, "Emanating Power and Specific Surface Area," *Radiation Protection Dosimetry*, vol. 7, pp. 73–76, 01 1984.

[23] G. NR, "Radon emanation from coals: effects of moisture and particle size," pp. 48(3):283–8., March 1985.

[24] J. Stajic and D. Nikezic, "Theoretical calculation of radon emanation fraction," *Nuclear Instruments and Methods in Physics Research Section B: Beam Interactions with Materials and Atoms*, vol. 336, pp. 19–25, 2014.